Stratigraphic, geochronological, and geochemical constraints on the genesis of Late Cretaceous volcanic rocks in the Sixtymile district of west central Yukon, Canada (NTS 116C/2, 115N/15)

Emilia Butty
Queen's Facility for Isotope Research, Department of Gological Sciences and Geological Engineering, Queen's University
Yukon Geological Survey

*Patrick J. Sack**
Yukon Geological Survey

Matthew Leybourne
Queen's Facility for Isotope Research, Department of Gological Sciences and Geological Engineering, Queen's University

James Crowley
Boise State University

Butty, E., Sack, P.J., Leybourne, M. and Crowley, J., 2026. Stratigraphic, geochronological, and geochemical constraints on the genesis of Late Cretaceous volcanic rocks in the Sixtymile district of west central Yukon, Canada (NTS 116C/2, 115N/15). *In*: Yukon Exploration and Geology 2025, A. Stuart, L.H. Weston and S.K. Schultz (eds.), Yukon Geological Survey, Government of Yukon, p. 91–117, plus digital appendices.

Abstract

In the Yukon, Late Cretaceous rocks are associated with significant porphyry systems that are of interest from mineral exploration, mineral potential and land use planning perspectives. The Sixtymile district of west-central Yukon contains rocks thought to be of this age, but their origin is largely unknown due to poor geochronological and geochemical constraints. In this contribution geologic mapping, U-Pb zircon geochronology, whole-rock geochemistry, and strontium (Sr), neodymium (Nd), and lead (Pb) whole-rock isotopes are used to characterize Late Cretaceous volcanic rocks in the Sixtymile district. Bedrock geology in the Sixtymile district is composed of a Yukon-Tanana terrane metamorphic basement overlain by undeformed and unmetamorphosed Cretaceous sedimentary and volcanic rocks. The Cretaceous rocks have a consistent stratigraphy consisting of a basal sedimentary unit, a middle andesitic unit, and an upper basaltic andesite unit. Four new U-Pb magmatic zircon ages that range between 69.779 ± 0.020 and 69.802 ± 0.020 Ma from the andesitic component of the volcanic stratigraphy demonstrate the volcanic event was short lived and lasted a maximum of 60 000 years. Late Cretaceous volcanic rocks are dominantly subalkaline and have continental arc geochemical signatures: 1) thorium/ytterbium (Th/Yb) versus niobium/ytterbium (Nb/Yb) values plot in the volcanic arc field; 2) extended trace element plots reveal negative Nb and titanium (Ti) anomalies and positive lead (Pb) anomalies; and 3) high field strength elements (HFSE) and light rare earth elements (LREE) are depleted compared to large ion lithophile elements (LILE). Additionally, isotope ratios reveal $^{87}Sr/^{86}Sr_i$ of 0.7050 to 0.7056, $^{143}Nd/^{144}Nd_i$ values of 0.5124 to 0.5126, εNd_i values of -1.9 to 1.1, and elevated Pb isotope ratios. We suggest that the Sixtymile district Late Cretaceous volcanic rocks are consistent with a relatively primitive continental magmatic arc setting.

* patrick.sack@yukon.ca

Plain language summary

This paper describes the geology of the Sixtymile district of western Yukon and presents data on the age of volcanic rocks from the area, and how the magmas that formed the volcanic rocks were generated. The geology of the Sixtymile district consists of a basement of metamorphic rocks overlain by sedimentary and volcanic rocks. The sedimentary and volcanic rocks were mostly preserved in a small basin (approximately 7 by 15 km) formed along the Sixtymile-Pika fault. The volcanic rocks in the Sixtymile district are 69.8 million years old and likely erupted in less than 60 000 years. The chemistry of the volcanic rocks suggests that they are the products of subduction-related magmatism.

Introduction

Late Cretaceous (ca. 84 to 68 Ma) volcanic rocks in the northern Cordillera are widely distributed southwest of the Tintina fault where they extend from northwestern British Columbia, through the Yukon and into Alaska (Fig. 1). Additionally, Late Cretaceous rocks are associated with significant porphyry systems (porphyry, epithermal and skarn deposits; Fig. 2) and are of interest from mineral exploration, mineral potential and land use planning perspectives. In the Yukon, these rocks include the Windy-Table, Open Creek, Tslansanlin and Carmacks group volcanic rocks which have mostly been investigated at regional mapping scales (1:50 000 to 1:250 000; e.g., Tempelman-Kluit, 1974, 1984, 2009; Grond et al., 1984; Mortensen, 1988, 1996; Ryan et al., 2013; Bordet et al., 2019). A few localized studies related to mineralization (Glasmacher and Friedrich, 1992; Smuk, 1999) or petrogenesis (Francis and Minarik, 2008) have also been completed.

It is generally recognized that a coarse conglomerate or breccia makes up the lowest Late Cretaceous stratigraphy followed by an andesitic volcanic and volcaniclastic package capped by basaltic flows and breccias (e.g., Payne et al., 1987; Johnston et al., 1996; Tempelman-Kluit, 2009). A shallowly dipping (<10˚) unconformity is locally recognized between the andesitic and basaltic components of the stratigraphy (e.g., Johnston et al., 1996; Francis and Minarik, 2008), but the entire volcanic package is thought to be genetically related and regionally flat lying. The current understanding of the magmatic setting and petrogenesis of these rocks is hampered by the lack of high quality, precise geochronological and geochemical control on the volcanic stratigraphy (e.g., Grond et al., 1984; Lowey et al., 1986). Partially based on these limited data, a continental arc magmatic setting has been ascribed to the more andesitic components of the stratigraphy (e.g., Morris et al., 2014), whereas a continental flood basalt, hot-spot related petrogenesis (Johnston et al., 1996) is primarily based on samples from the upper basaltic rocks.

One of the locales in the Yukon with Late Cretaceous magmatic rocks is the Sixtymile district along the Yukon-Alaska border (Mortensen, 1988, 1996; Rimando et al., 2022). In this area, Late Cretaceous volcanic rocks are primarily found within a pull-apart graben formed at a stepover along the orogen-normal, Cretaceous Sixtymile-Pika fault system (Fig. 2; Mortensen, 1996; Allan et al., 2017). The area has been regionally mapped (1:50 000 and 1:250 000; Mortensen, 1988; 1996), but the Late Cretaceous volcanic rocks have not been characterized in detail, and prior to this study, were undated. This paper describes the Late Cretaceous geology of the Sixtymile district in detail and reports four new chemical abrasion-isotope dilution-thermal ionization mass spectrometry (CA-TIMS) U-Pb ages for volcanic strata along with 27 whole-rock lithogeochemical analyses and six whole-rock Sr, Nd and Pb isotope analyses. We use this new data to constrain the stratigraphy for the Sixtymile district and interpret a continental magmatic arc origin for the volcanic rocks.

Regional geology

The bedrock geology of the Sixtymile district consists of metamorphic basement overlain by Cretaceous volcanic and sedimentary rocks (Mortensen, 1988, 1996) dissected by the 130 km-long Sixtymile-Pika fault system (Allan et al., 2017). The metamorphic basement is primarily of Yukon-Tanana terrane affinity; however, towards the southern margin of the district, the Fiftymile fault, a low-angle extensional fault, juxtaposes the Fiftymile batholith of autochthonous North American affinity against the parautochthonous Yukon-Tanana terrane rocks (Fig. 3, Mortensen, 1996; Dusel-Bacon and Mortensen, 2024).

Yukon-Tananaterranehasalowermostmetasedimentary assemblage of parautochthonous North American affinity (Snowcap assemblage) overlain by up to three volcanic arc or back-arc packages separated by unconformities (Finlayson, Klinkit and Klondike

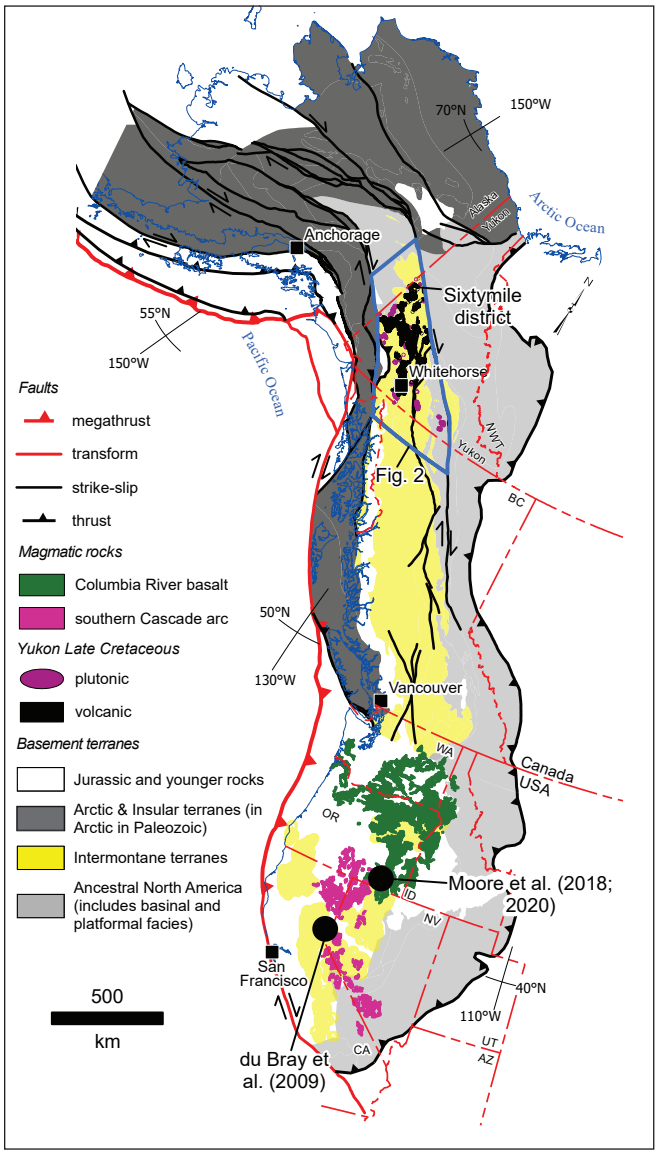

Figure 1. *Tectonic realms of the northern North American Cordillera (modified after Colpron et al., 2007). Continental USA geology from Garrity and Soller (2009). Black dots represent the location of the du Bray et al. (2009) and Moore et al. (2018 and 2020) studies. Figure 2 is delineated by blue outline.*

assemblages, respectively; Colpron et al., 2006; Dusel-Bacon et al., 2006). In the Sixtymile district, only the Finlayson and Klondike assemblages are recognized (Fig. 3). Locally, the Finlayson assemblage is a mix of quartzose and graphitic metasedimentary rocks and Mississippian micaceous schist of metavolcanic origin (Nasina assemblage of Mortensen, 1988) and coeval intermediate composition orthogneiss of the Simpson Range suite. The Klondike assemblage is a Permian meta-igneous package of felsic schist (Mortensen, 1988). There are also a few slivers of ultramafic rocks near the margins of a thrust-bound package of the Klondike assemblage (Fig. 3).

The majority of $^{40}Ar/^{39}Ar$ analyses of biotite and muscovite for the Sixtymile district are Early to Middle Jurassic and are associated with exhumation from mid-crustal levels during initial accretion of the Yukon-Tanana terrane with the western margin of North America (Johnston and Erdmer, 1995; Colpron et al., 2022; Colpron et al., 2025). Following exhumation to upper crustal levels, domains with mid-Cretaceous $^{40}Ar/^{39}Ar$ cooling ages formed in autochthonous rocks with Late Devonian intrusions such as the Fiftymile batholith (Dusel-Bacon et al., 2002; Dusel-Bacon and Mortensen, 2024). These mid-Cretaceous cooling domains are interpreted as windows through the upper parautochthonous Yukon-Tanana plate into the lower autochthonous North American plate (e.g., Staples et al., 2016). Coeval with mid-Cretaceous extension was the deposition of the Indian River Formation, a succession of pebble conglomerate, sandstone, siltstone and ash-fall tuff up to 500 m thick (Lowey, 1984). After deposition of the mid-Cretaceous Indian River Formation, Late Cretaceous volcanic and sedimentary rocks such as those in the Sixtymile district were deposited. Cretaceous and younger deformation in the Sixtymile region was brittle in nature and is dominated by the northeast-striking Sixtymile-Pike fault zone that extends from the Denali fault to the Tintina fault and accommodates up to 17 km of sinistral displacement (Allan et al., 2017). The Sixtymile-Pika fault also appears to have influenced the emplacement, and/or preservation of the Late Cretaceous magmatic rocks in the area (Allan et al., 2013).

Local geology

Thirty days of geological mapping (1: 25 000 scale) were conducted in 2023 and 2024 in the Sixtymile district (Figs. 3 to 5). Access to the Sixtymile district is from the Top of the World Highway. Mapping was conducted via foot-traverses, and access was by truck and all-terrain vehicles. The Sixtymile district was not glaciated in the Quaternary (Duk-Rodkin, 1996) and the landscape consists of rolling hills separated by over-steepened valleys with thick forest coverage and relatively deep weathering, all of which result in poor bedrock exposure. Because of the poor bedrock exposure, changes in felsenmeer composition are used to map the approximate location of contacts. Additionally, a few key man-made exposures in quarry pits and placer excavations also help determine relationships between units.

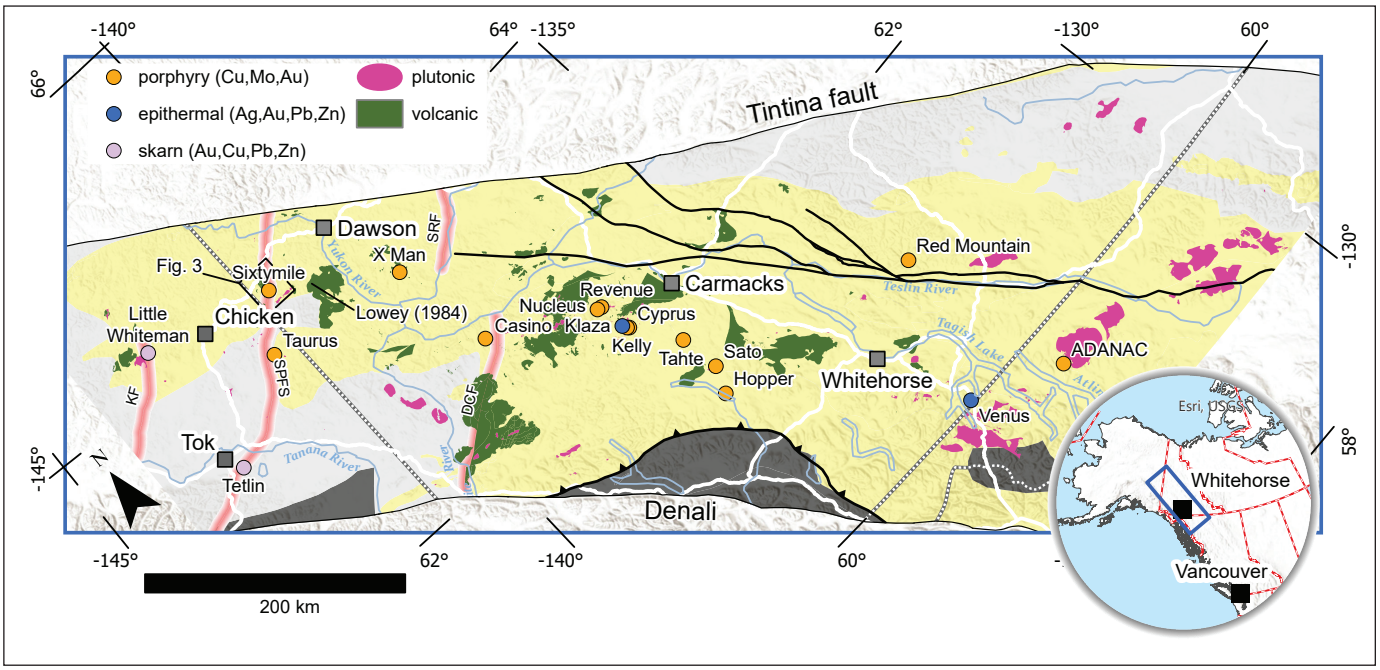

Figure 2. *Simplified bedrock geology map of eastern Alaska, southwest Yukon and northeast British Columbia, including Cretaceous-orogen normal faults (red lines: Ketchumstuk fault (KF); Sixtymile-Pika fault system (SPFS); Stewart River fault (SRF); and Dip Creek fault (DCF)), as well as Late Cretaceous magmatic rocks and mineral occurrences (modified from Allan et al., 2017). Basement terrane colours same as Figure 1.*

Metamorphic basement

The Sixtymile district basement geology is comprised of metamorphic rocks (Figs. 3 and 6). The oldest of these consist of the Late Devonian Grass Lakes suite, which is a coarse-grained, foliated granodiorite with rounded plagioclase crystals up to 3–5 cm in diameter. These intrusions are found on the southern boundary of the map area (Dusel-Bacon and Mortensen, 2024). Most of the district is underlain by Late Devonian to Early Mississippian quartzite and metavolcanic rocks of the Finlayson assemblage and their coeval metaplutonic equivalent, the Simpson Range suite. The quartzite is white to dark grey, thinly to thickly layered, and contains carbonaceous foliations. The metavolcanic rocks are pale green and include chlorite and quartz-rich layers (Fig. 6g). The metaplutonic rocks are equigranular, foliated, hornblende-bearing and of granodiorite composition. The youngest basement units are mostly found in a thrust-bound panel of Permian, silver-grey, muscovite-chlorite-quartz schists of the Klondike assemblage, and small lozenges of red-brown weathering ultramafic rocks of the Dawson-Clinton Creek assemblage (Mortensen, 1988).

Late Cretaceous conglomerate

The stratigraphically lowest rocks investigated in detail in this study are a sedimentary unit that overlies the metamorphic basement and consists of unmetamorphosed, poorly consolidated sedimentary rocks. These rocks weather easily and are poorly preserved, and most exposures occur in road and placer workings; a few natural exposures are found near the Top of the World highway and to the north in creek banks and confluences. Where observed in outcrop, this unit is dominated by matrix to clast-supported, pebble to cobble conglomerate with a sandy matrix (Fig. 6h). The sandstone matrix is white-beige in colour and grains are 0.1 to 0.3 mm in diameter. The clasts are rounded to subrounded, black, white and beige in colour, and 0.5 mm to >5 cm in diameter. The lithologies are metamorphic and quartz in composition. At the confluence of Little Gold and Big Gold creeks, an extensive excavation 3 m high exposes a section that includes a spheroidal-weathering, coarse-grained sandstone, a thin coal seam, a 15 cm-thick tuff unit, as well as the matrix-supported pebble conglomerate. The tuff is light grey, very fine-grained and has quartz eyes and biotite phenocrysts. Higher in the Late Cretaceous stratigraphy, there are minor occurrences of coarse-sandstone; the best exposures of which are along the Sixtymile road.

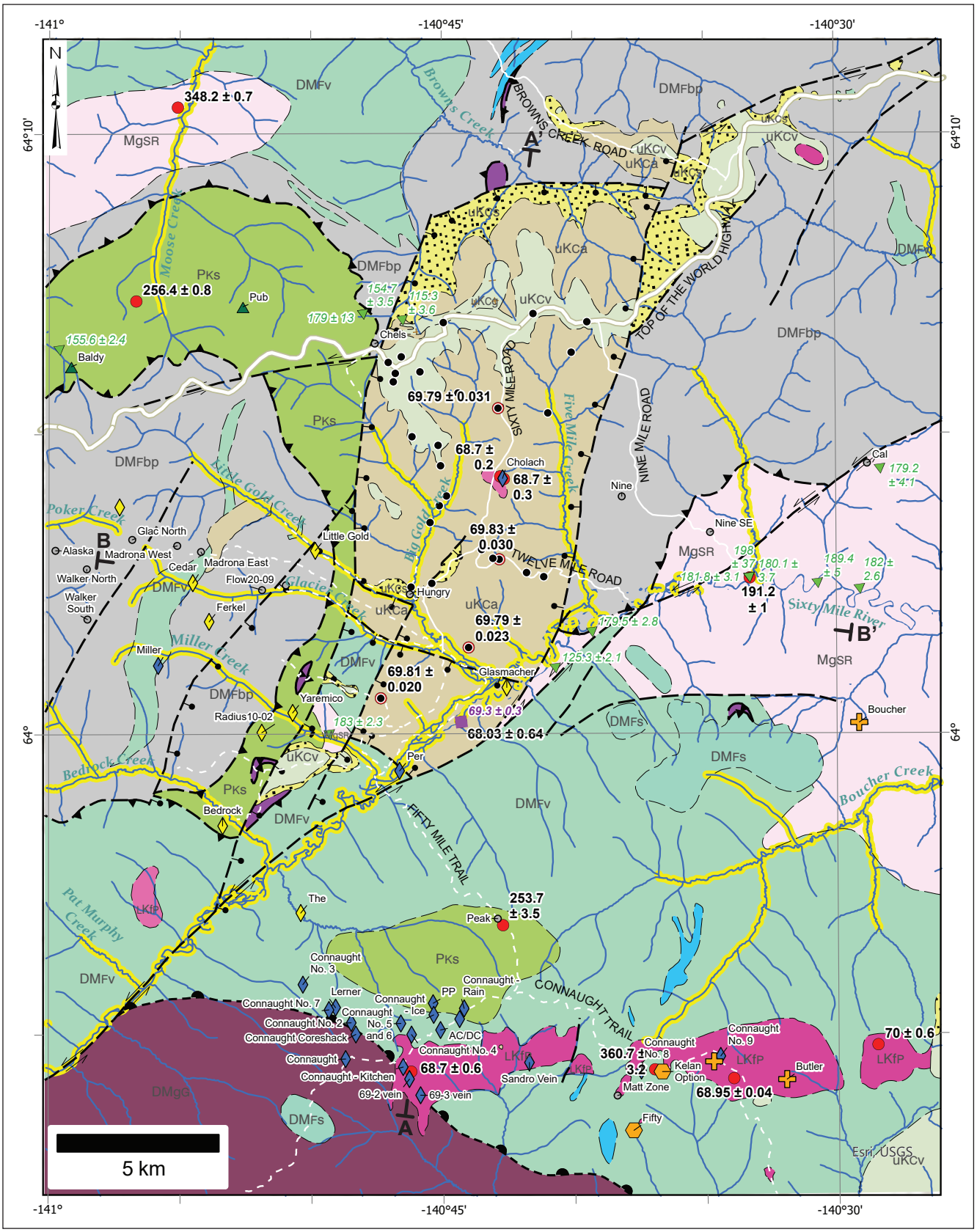

Figure 3. *Bedrock geology map of the Sixtymile district. See legend on following page (Sack et al., in prep).*

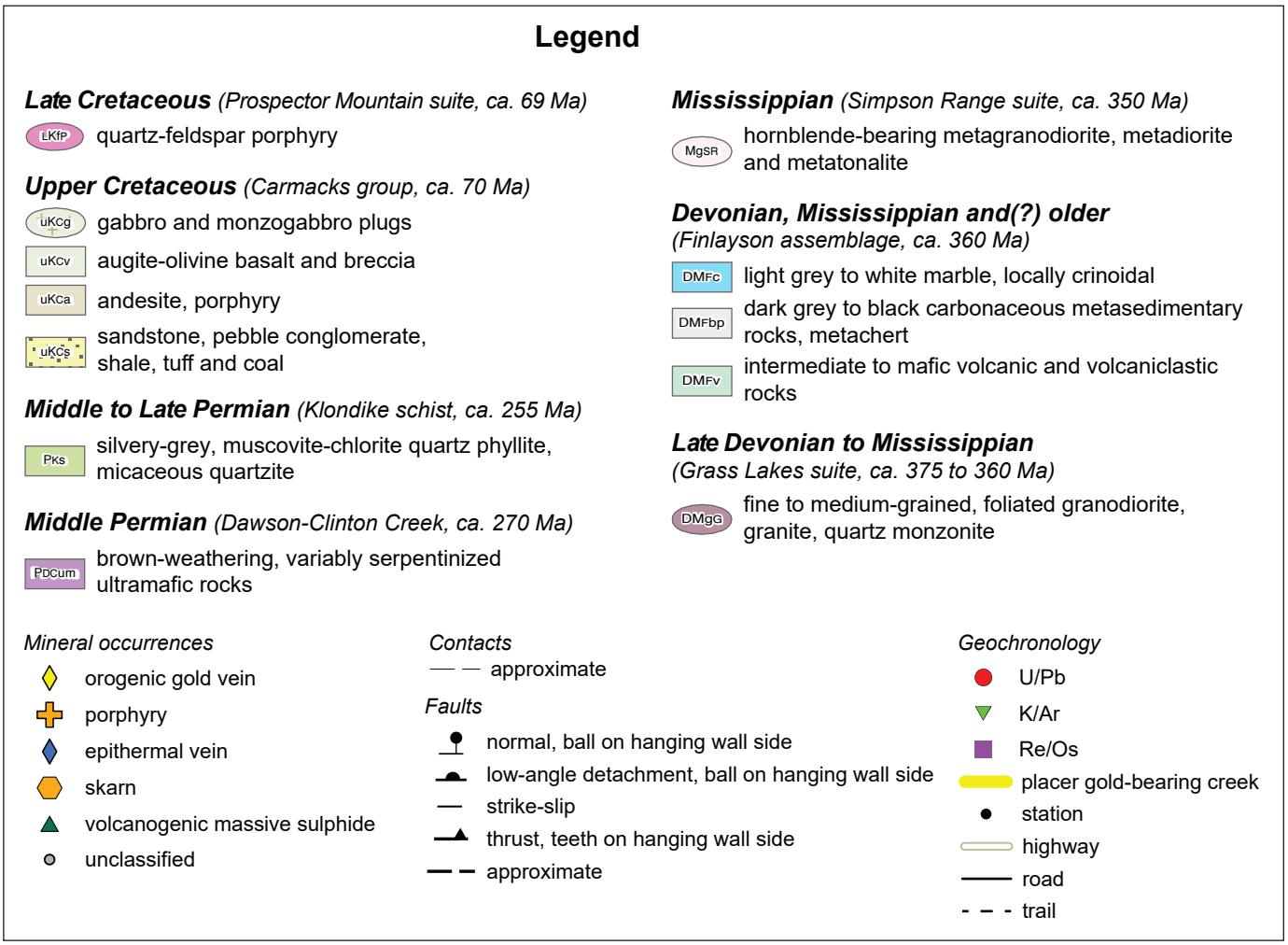

Figure 3 (legend). *Bedrock geology map of the Sixtymile district (Sack et al., in prep).*

Late Cretaceous volcanic rocks

Andesitic rocks

The most widespread unit reported in detail in this study is an unfoliated andesitic unit. This unit is typically found immediately above the basal conglomerate from approximately 670 to 980 m elevation and is approximately 300 m thick. It extends from near the Top of the World Highway, south to the Sixtymile River (Fig. 3), and constitutes most of the rocks exposed within the graben. The andesitic rocks are massive flows, crystal tuffs, and block and ash flows (Fig. 6a,e). They are light to dark grey and contain plagioclase ± hornblende, biotite, quartz and pyroxene phenocrysts. The phenocrysts in the andesite unit are primarily plagioclase (≤80%), and subordinate amounts of hornblende (≤15%) and biotite (≤5%) in a plagioclase-rich matrix (Fig. 7a-h). In rare samples, quartz phenocrysts are visible in thin section where they make up to 5% of the rock. The plagioclase phenocrysts vary in size from 0.5–2 mm near the top of the succession, to 2–3 mm near the bottom. Trace pyroxene phenocrysts are seen near the top of the unit, but not in the lower stratigraphy. Hornblende and biotite phenocrysts range from <1–2 mm in diameter. Progressing down section, the plagioclase and hornblende phenocrysts increase in size and abundance. Biotite is limited to the lower sections of the succession.

Basaltic andesitic rocks

The upper basaltic andesite unit is at least 200 m thick and found at higher elevations (≥980 m) in the northern part of the study area around the Top of the World Highway (Fig. 3). The basaltic andesite unit is unfoliated, dense, dark grey to black on fresh surfaces, and weathers dark brown (Fig. 6d). It is

generally massive, but surfaces can show differential weathering with a pseudo-fragmental texture suggestive of a monomictic breccia. Plagioclase phenocrysts are 0.5–1 mm and surrounded by an aphanitic groundmass; in some samples, small pyroxene crystals (<0.5 mm) are observed (Fig. 7e). The phenocrysts are dominantly plagioclase (80%) with subordinate amounts of pyroxene (7%), hornblende (5%), olivine (3%) and opaque minerals (probably magnetite; 5%). Hornblende, biotite and quartz are very fine-grained and only identifiable in thin section (Fig. 7a–f).

Late Cretaceous(?) intrusive rocks

Three types of intrusive rocks crosscut the Late Cretaceous volcanic rocks. Hornblende-biotite granodiorite and hornblende diorite intrude the andesitic unit in drill core in the Sixtymile valley near the Per occurrence, as well as basement units along the southern margin of the map near the Connaught occurrences (Fig. 3). These intrusions are associated with porphyry mineralization (Allan et al., 2017). Pyroxene porphyritic gabbro to monzogabbro bodies intrude the andesitic and basaltic andesite units at higher elevations. These intrusions weather brown-red and have up to 25% equant pyroxene, 7–10 mm in size, in an aphanitic groundmass (Fig. 6f). Dense, dark green to black aphanitic mafic dykes crosscut the andesitic unit (Fig. 6e). These dykes can have small pyroxene phenocrysts less than 0.2 mm in diameter and resemble the basaltic andesite unit implying they could be feeder dykes to that unit.

Methods

Analytical methods are briefly summarized here and are described in more detail in Appendices A and B. Geochronological data were collected at Boise State University using laser ablation-inductively coupled plasma mass spectrometry (LA-ICPMS) and chemical abrasion-isotope dilution-thermal ionization mass spectrometry (CA-TIMS) of U-Th-Pb in zircon. Whole-rock geochemical analyses were done by Analytical Laboratory Services (ALS) Geochemistry on samples prepared with a mild steel mill and analyzed with X-ray fluorescence spectroscopy (XRF) and ICPMS after fusion and four acid digestion. Whole-rock pulps were also analyzed at the University of Melbourne for Sr, Nd, Pb isotope compositions.

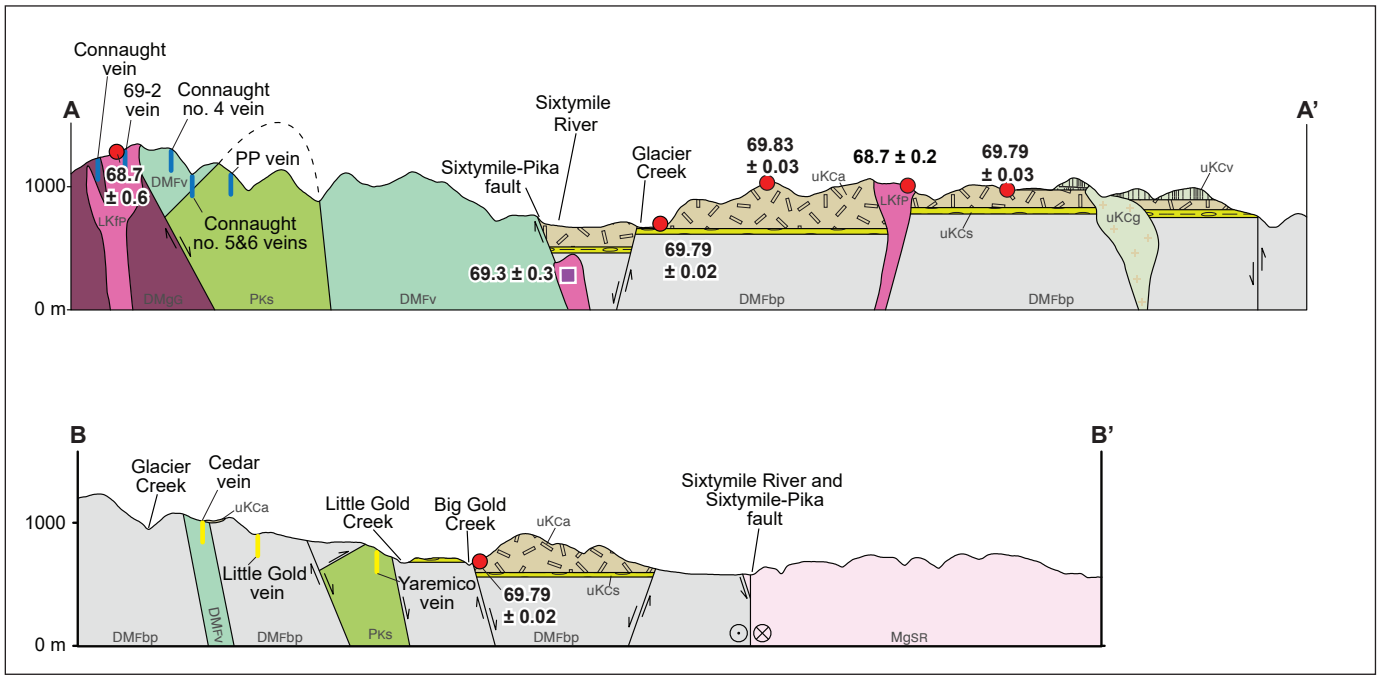

Figure 4. *Long-section (A–A') and cross-section (B–B') through the Sixtymile district. Section locations shown on Figure 3. Legend same as Figure 3. Three times vertical exaggeration.*

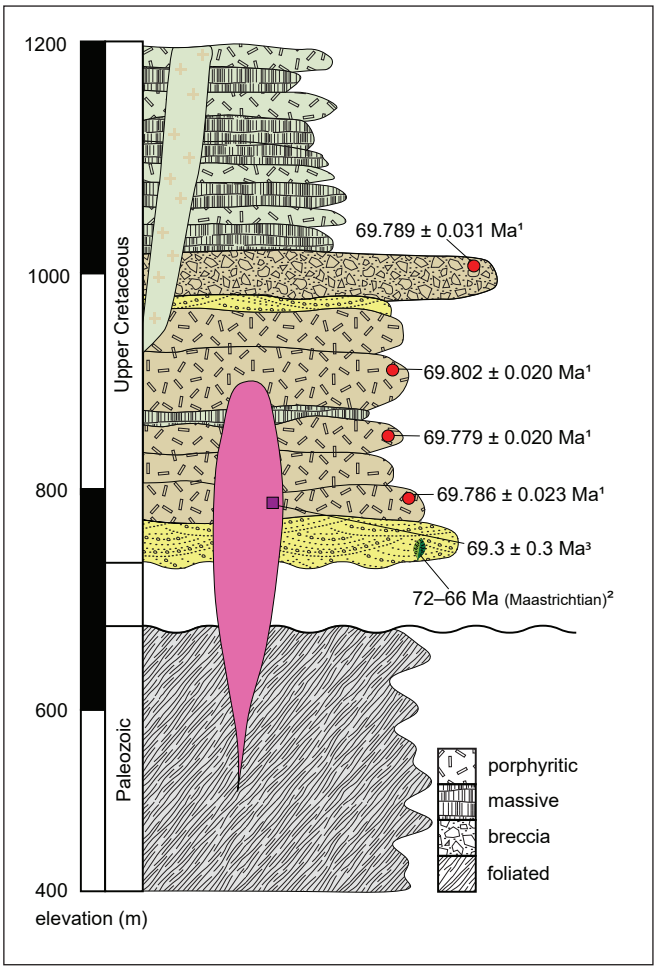

Figure 5. *Cretaceous stratigraphy of the Sixtymile district. Colours and age symbols same as Figure 3. Superscripts on age dates are as follows: 1 – this study; 2 – Lowey (1984); 3 – Allan et al. (2017).*

Results

Geochronology

New geochronological data tightly constrain the age of Late Cretaceous magmatism in the Sixtymile district. Four samples from throughout the Late Cretaceous volcanic stratigraphy were analyzed for U-Pb LA-ICPMS and CA-TIMS zircon geochronology. All dates and ages are 206Pb/238U unless otherwise stated. Data for cathodoluminescence (CL) imaging and LA-ICPMS analyses are in Appendix A. Chemical abrasion-thermal ionization mass spectrometry data are in Table 1.

Sample 23PS053-1 is a pink-orange weathering plagioclase porphyritic andesite collected from a hilltop on Twelve Mile Road (Fig. 3) near the middle of the andesitic unit (Fig. 5). This sample yielded three populations of zircon: Paleozoic to Mesozoic, mid-Cretaceous, and Late Cretaceous (Fig. 8; Appendix A). The Paleozoic to Mesozoic population is dark in CL and displays oscillatory zoning; grains are elongate (≥3:1 aspect ratio), and have LA-ICPMS dates between 368 and 207 Ma. The mid-Cretaceous grains are stubby (≤2:1 aspect ratio), rounded, display moderate brightness with sector zoning, and have LA-ICPMS dates between 119 and 95 Ma. The Late Cretaceous population of grains display dark to moderate lightness in CL, are elongate with sharp crystal faces, and have LA-ICPMS dates between 73.5 and 65.0 Ma. The Paleozoic to Mesozoic and mid-Cretaceous grains are interpreted to be inherited, whereas the Late Cretaceous grains are interpreted as volcanic in origin. The weighted mean age of 18 Late Cretaceous LA-ICPMS analyses is 69.4 ± 0.7 Ma; the oldest three Late Cretaceous grains are interpreted to be antecrysts, and the youngest two grains are believed to have undergone minor Pb-loss. Six zircon grains analyzed by CA-TIMS yielded concordant $^{206}Pb/^{238}U$ dates that range from 69.845 ± 0.050 to 69.771 ± 0.040 Ma (Table 1); all six grains have a weighted mean age of 69.802 ± 0.020 Ma (MSWD = 1.5, probability of fit = 0.19, n = 6/6). The weighted mean age of 69.802 ± 0.020 Ma is interpreted as the crystallization age of this sample.

Sample 23PS004-2 is a medium grey to brown andesitic block and ash pyroclastic rock (Fig. 6a and Fig. 9) located near the top of the andesite unit (Fig. 5) in a quarry pit on the main Sixtymile access road (Fig. 3). This sample yielded three populations of zircon: Paleozoic to Mesozoic, mid-Cretaceous and Late Cretaceous (Fig. 10; Appendix A). The Paleozoic to Mesozoic population yields elongate (≥3:1 aspect ratio), euhedral to subhedral zircons that exhibit various CL zoning (sector, concentric and rim/core relationships), and have LA-ICPMS dates between 356 and 205 Ma. The mid-Cretaceous population yields stubby to elongate subhedral grains displaying sector CL zoning, and have LA-ICPMS dates between 113 and 100 Ma. The Late Cretaceous population yields elongate (≥3:1 aspect ratio), euhedral zircons exhibiting weak to no CL zoning, and have LA-ICPMS dates between 72.6 and 68.2 Ma. The Paleozoic to Mesozoic and mid-Cretaceous grains are interpreted to be inherited, whereas the Late Cretaceous grains are interpreted as volcanic in origin. The weighted mean $^{206}Pb/^{238}U$ age of the four youngest LA-ICPMS analyses is

68.7 ± 1.2 Ma. Four zircon grains analyzed by CA-TIMS yielded concordant $^{206}Pb/^{238}U$ dates between 169.806 ± 1.246 and 69.781 ± 0.051 Ma (Table 1) and have a weighted mean age for the three youngest of 69.789 ± 0.031 Ma (MSWD = 0.2, probability of fit = 0.86, n = 3/4). The weighted mean age of 69.789 ± 0.031 Ma is interpreted as the crystallization age of this sample.

Sample 23PS064-1 is a green-brown andesitic crystal tuff (Figs. 6b and 11) located near the bottom of the andesite unit (Fig. 5), 2 km northwest of the mouth of Big Gold Creek (Fig. 3). This sample yielded four populations of zircon: Paleoproterozoic, Paleozoic to Mesozoic, mid-Cretaceous and Late Cretaceous (Fig. 11; Appendix A). A single stubby, rounded zircon was analyzed and displayed a moderate CL response, and has a Paleoproterozoic

Figure 6. *Field photographs of select outcrops and hand samples:* **(a)** *pyroclastic breccia;* **(b)** *crystal tuff;* **(c)** *massive plagioclase porphyritic andesite;* **(d)** *plagioclase porphyritic basaltic andesite;* **(e)** *mafic dike cross-cutting andesitic block and ash flow; quarry face is approximately 3 m high;* **(f)** *pyroxene porphyritic monzogabbro;* **(g)** *chlorite-muscovite-quartz schist; and* **(h)** *pebble conglomerate.*

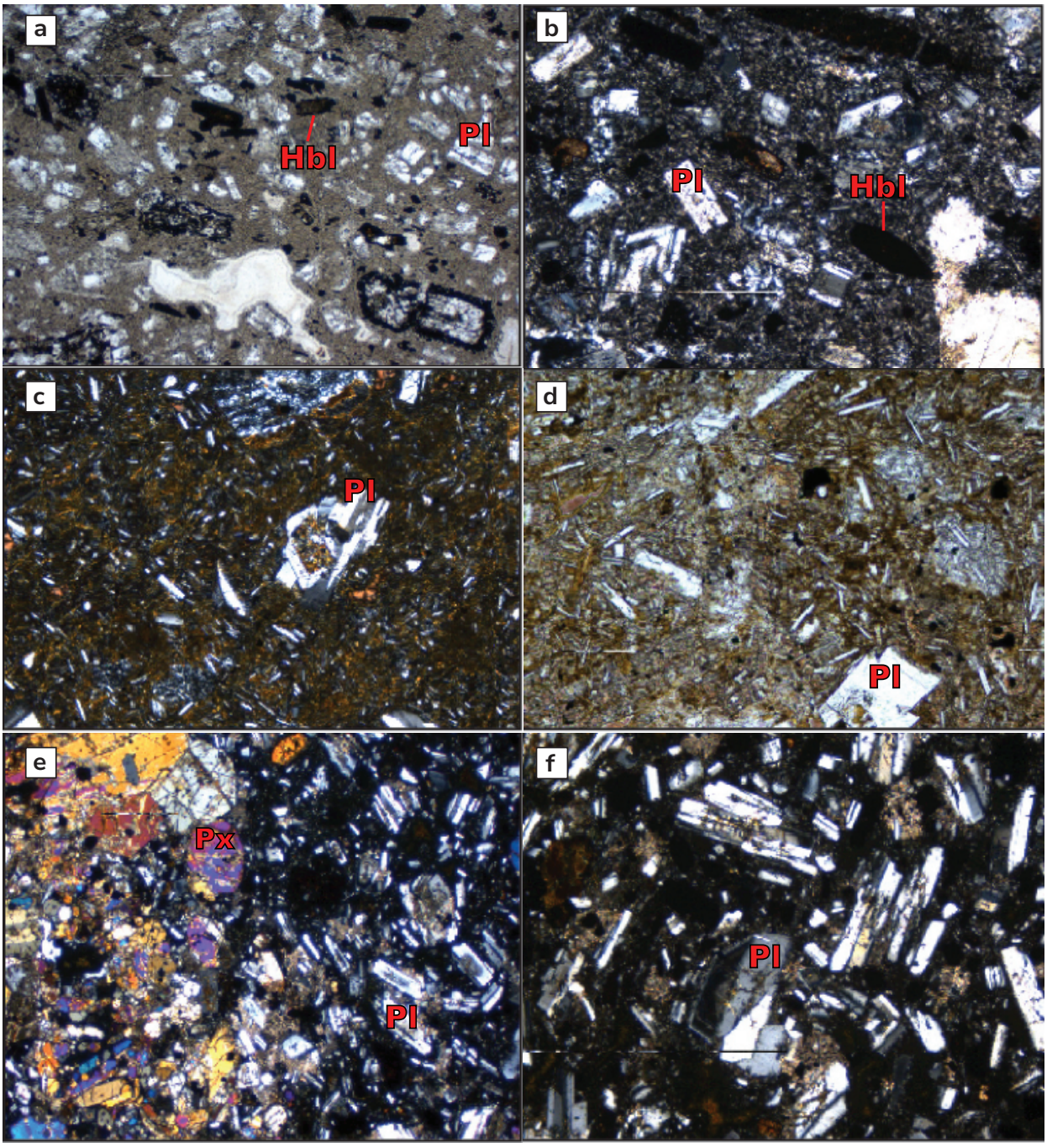

Figure 7. *Photomicrographs of select samples:* **(a)** *23PS017-1 (plagioclase, quartz, hornblende andesite porphyry) in plane polarized light (PPL) at 2.5x magnification and field of view (fov) is 10 mm across;* **(b)** *23PS017-1 in cross-polarized light (XPL) at 5x magnification and fov is 5 mm across;* **(c)** *23PS038-1 (plagioclase, hornblende, biotite andesite porphyry) in XPL at 5x magnification (fov 5 mm across);* **(d)** *23PS038-1 in XPL at 10x magnification and fov is 2.5 mm across;* **(e)** *23PS006-1 (plagioclase, pyroxene basaltic andesite) in XPL at 10x magnification (fov 2.5 mm across); and* **(f)** *23PS006-1 in XPL at 5x magnification (fov 5 mm across). Mineral abbreviations from Whitney and Evans (2010); Hbl – hornblende; Pl – plagioclase; Px – pyroxene.*

Table 1. CA-TIMS U-Pb zircon data table.

								Radiogenic Isotope Ratios										Isotopic Dates									
Sample	LA-ICPMS label	Th / U	$^{206}Pb^*$ x10^{-13} mol	mol % $^{206}Pb^*$	Pb* (pg)	Pb_c (pg)	Pb* / Pb_c	$^{206}Pb/^{204}Pb$	$^{208}Pb/^{206}Pb$	$^{207}Pb/^{206}Pb$	% err	$^{207}Pb/^{235}U$	% err	$^{206}Pb/^{238}U$	% err	corr. coef.	$^{207}Pb/^{206}Pb$	±	$^{207}Pb/^{235}U$	±	$^{206}Pb/^{238}U$	±	include in weighted mean?	*Weighted mean calculations (2 sigma errors)*		
(a)		(b)	(c)	(c)	(c)	(c)	(c)	(d)	(e)	(e)	(f)	(e)	(f)	(e)	(f)		(g)	(f)	(g)	(f)	(g)	(f)				
23PS053-1																										
z5	67	0.306	0.6068	99.77%	14	0.12	121	7701	0.098	0.047525	0.114	0.071351	0.170	0.010894	0.072	0.8724	74.6232	2.707	69.981	0.115	69.845	0.050	x	$^{206}Pb/^{238}U$ ± random (+tracer) [+decay constant]	MSWD =	1.48
z3	60	0.595	1.5704	99.91%	40	0.12	342	20069	0.191	0.047503	0.076	0.071301	0.138	0.010891	0.072	0.9369	73.5253	1.815	69.933	0.093	69.828	0.050	x	**69.802 ± 0.02 (0.03) [0.08]**	pof =	0.19
z1	55	0.615	1.6259	99.91%	42	0.13	326	19028	0.197	0.047472	0.087	0.071235	0.147	0.010888	0.071	0.9232	71.9517	2.074	69.871	0.099	69.810	0.049	x		n =	6
z2	74	0.749	1.1910	99.81%	32	0.19	169	9554	0.240	0.047468	0.089	0.071216	0.148	0.010886	0.071	0.9173	71.7443	2.11	69.853	0.1	69.797	0.050	x			
z4	62	0.696	1.7114	99.91%	45	0.13	353	20169	0.223	0.047468	0.070	0.071198	0.135	0.010883	0.072	0.9578	71.7765	1.672	69.836	0.091	69.779	0.050	x			
z6	69	0.400	0.2804	99.44%	7	0.13	52	3219	0.128	0.047472	0.167	0.071195	0.239	0.010882	0.057	1.2279	71.9446	3.96	69.833	0.161	69.771	0.040	x			
23PS004-2																										
z5	63	0.318	0.4564	99.54%	10.9	0.18	62	3918	0.101	0.052017	0.230	0.191344	0.789	0.026691	0.743	0.957	285.12	5.27	177.78	1.29	169.806	1.246		$^{206}Pb/^{238}U$ ± random (+tracer) [+decay constant]	MSWD =	0.2
z4	54	0.933	1.7496	99.90%	48.6	0.14	347	18693	0.299	0.047407	0.079	0.071128	0.140	0.010887	0.072	0.930	68.72	1.88	69.77	0.09	69.800	0.050	x	**69.789 ± 0.031** (0.037) [0.084]	pof =	0.86
z3	70	0.719	0.1747	99.01%	4.6	0.15	32	1814	0.230	0.047568	0.444	0.071354	0.493	0.010884	0.090	0.616	76.78	10.54	69.98	0.33	69.785	0.062	x		n =	3
z2	62	0.897	0.3578	99.55%	9.9	0.14	73	3976	0.288	0.047345	0.189	0.071015	0.240	0.010884	0.073	0.792	65.57	4.49	69.66	0.16	69.781	0.051	x			
23PS064-1																										
z6	99	0.321	0.6690	98.48%	15.9	0.85	19	1200	0.103	0.050850	0.265	0.135954	0.315	0.019400	0.077	0.721	233.02	6.11	129.43	0.38	123.860	0.095		$^{206}Pb/^{238}U$ ± random (+tracer) [+decay constant]	MSWD =	0.8
z2	88	1.448	2.1386	99.86%	66.8	0.25	264	12676	0.464	0.047387	0.094	0.071110	0.152	0.010888	0.071	0.908	67.70	2.23	69.75	0.10	69.812	0.049	x	**69.786 ± 0.023** (0.031) [0.082]	pof =	0.55
z5	102	0.549	0.2238	98.43%	5.6	0.30	19	1149	0.176	0.047558	0.426	0.071358	0.478	0.010887	0.083	0.691	76.29	10.11	69.99	0.32	69.803	0.058	x		n =	5
z1	85	1.124	1.9507	99.89%	56.7	0.19	306	15753	0.360	0.047447	0.079	0.071176	0.140	0.010885	0.072	0.930	70.70	1.89	69.81	0.09	69.789	0.050	x			
z3	91	0.836	0.3998	99.34%	10.9	0.22	49	2743	0.268	0.047522	0.213	0.071269	0.261	0.010882	0.076	0.729	74.47	5.06	69.90	0.18	69.769	0.053	x			
z4	82	0.955	1.4756	99.81%	41.2	0.23	180	9680	0.306	0.047472	0.085	0.071184	0.146	0.010880	0.071	0.928	71.96	2.02	69.82	0.10	69.760	0.050	x			
23PS074-1																										
z3	110	0.817	1.0300	99.85%	28	0.12	223	12358	0.262	0.047458	0.064	0.071203	0.138	0.010886	0.072	1.026	71.25	1.51	69.84	0.09	69.799	0.050	x	$^{206}Pb/^{238}U$ ± random (+tracer) [+decay constant]	MSWD =	0.7
z6	106	0.931	1.1037	99.86%	31	0.13	233	12596	0.298	0.047482	0.086	0.071232	0.147	0.010885	0.073	0.923	72.47	2.04	69.87	0.10	69.792	0.051	x	**69.779 ± 0.020 (0.03) [0.08]**	pof =	0.62
z4	107	0.757	1.1416	99.89%	30	0.10	297	16710	0.243	0.047473	0.081	0.071211	0.142	0.010884	0.071	0.934	72.01	1.92	69.85	0.10	69.785	0.050	x		n =	6
z1	111	0.752	1.2895	99.91%	34	0.09	370	20852	0.241	0.047453	0.077	0.071178	0.139	0.010884	0.072	0.935	71.03	1.82	69.82	0.09	69.782	0.050	x			
z7	121	0.645	0.7973	99.82%	21	0.12	176	10201	0.207	0.047505	0.092	0.071253	0.153	0.010883	0.071	0.929	73.60	2.19	69.89	0.10	69.779	0.049	x			
z2	112	0.765	2.1006	99.93%	56	0.13	434	24384	0.245	0.047465	0.070	0.071152	0.134	0.010877	0.072	0.953	71.61	1.66	69.79	0.09	69.739	0.050	x			

(a) z1, z2, etc. are labels for analyses composed of single zircon grains that were annealed and chemically abraded (Mattinson, 2005).

(b) Model Th/U ratio calculated from radiogenic $^{208}Pb/^{206}Pb$ ratio and $^{207}Pb/^{235}U$ date.

(c) Pb* and Pbc are radiogenic and common Pb, respectively. mol % $^{206}Pb^*$ is with respect to radiogenic and blank Pb.

(d) Measured ratio corrected for spike and fractionation only. Pb fractionation correction for analyses done with tracer solution BSU1B is 0.16 ± 0.03 (1 sigma) %/amu (atomic mass unit) for single-collector Daly analyses, based on recent analyses of EARTHTIME ^{202}Pb-^{205}Pb ET2535 tracer solution.

(e) Corrected for fractionation and spike. Common Pb in zircon analyses is assigned to procedural blank with composition of $^{206}Pb/^{204}Pb$ = 18.04 ± 0.61%; $^{207}Pb/^{20}4Pb$ = 15.54 ± 0.52%; $^{208}Pb/^{204}Pb$ = 37.69 ± 0.63% (1 sigma). $^{206}Pb/^{238}U$ and $^{207}Pb/^{206}Pb$ ratios corrected for initial disequilibrium in $^{230}Th/^{238}U$ using a $D_{(Th/U)}$ of 0.20 ± 0.05 (1 sigma).

(f) Errors are 2 sigma, propagated using algorithms of Schmitz and Schoene (2007) and Crowley et al. (2007).

(g) Calculations based on the decay constants of Jaffey et al. (1971). $^{206}Pb/^{238}U$ and $^{207}Pb/^{206}Pb$ dates corrected for initial disequilibrium in $^{230}Th/^{238}U$ using a $D_{(Th/U)}$ of 0.20 ± 0.05 (1 sigma).

core ($^{207}Pb/^{206}Pb$ date of 1837 ± 44 Ma). The Paleozoic to Mesozoic population yields stubby to elongate (1:1 to 3:1 aspect ratio) euhedral zircons with mainly sector and core zoning, and having LA-ICPMS dates between 382 and 153 Ma. The mid-Cretaceous population yields mostly stubby (≤2:1 aspect ratio), rounded zircons with varied CL zoning (weak to none, sector), and LA-ICPMS dates between 121 and 97 Ma. The Late Cretaceous population yields euhedral zircons with various CL zoning (weak to none, sector, oscillatory), and are mostly elongate (≥3:1 aspect ratio); LA-ICPMS dates range between 77.0 and 65.4 Ma. The Paleoproterozoic, Paleozoic to Mesozoic and mid-Cretaceous grains are interpreted to be inherited, whereas the Late Cretaceous grains are interpreted as volcanic in origin. The weighted mean $^{206}Pb/^{238}U$ age of the 24 youngest LA-ICPMS analyses is 69.1 ± 0.9 Ma. Six zircon grains analyzed by CA-TIMS yielded concordant $^{206}Pb/^{238}U$ dates between 123.860 ± 0.095 and 69.760 ± 0.050 Ma (Table 1), and have a weighted mean age for the four youngest of 69.786 ± 0.023 Ma (MSWD = 0.8, probability of fit = 0.55, n = 5/6). The weighted mean age of 69.786 ± 0.023 Ma is interpreted as the crystallization age of this sample.

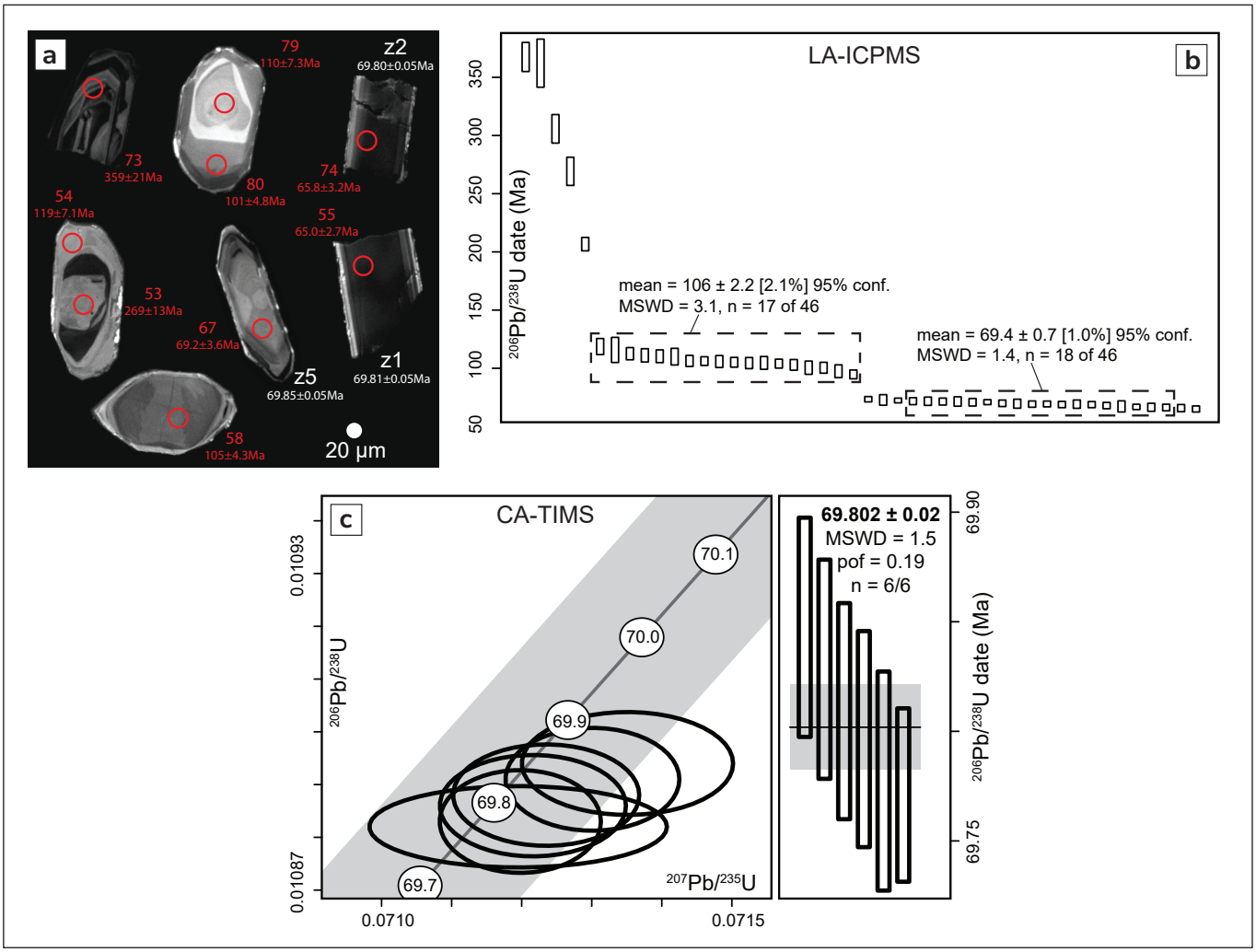

Figure 8. *Sample 23PS053-1 U-Pb geochronological results.* ***(a)*** *Cathodoluminescence images of representative igneous zircons. Red labels indicate LA-ICPMS analysis number and age with associated error; the red open circle indicates the location of the analysis spot; white analysis number and age with associated error refers to grain analyzed by CA-TIMS.* ***(b)*** *Ranked plot of LA-ICPMS $^{206}Pb/^{238}U$ dates.* ***(c)*** *Concordia diagram (left) and ranked $^{206}Pb/^{238}U$ dates (right) for zircons analyzed by CA-TIMS. Grey horizontal bar shows calculated weighted mean with error. Analyses included in weighted mean age calculations (light grey horizontal bar) are bold; analyses with thin lines are not used in calculations. The light grey band around Concordia (dark grey line) shows the decay constant uncertainties. Errors in all plots are at 2σ. MSWD – mean squared weighted deviation; pof - probability of fit; n – number of analyses included in age calculation.*

Sample 23PS074-1 is a purple-weathering, plagioclase porphyritic andesite collected on the ridge between Miller and Glacier creeks (Fig. 3), near the middle of the andesitic unit (Fig. 5). This sample yields mostly Late Cretaceous zircon with one Paleozoic grain and three mid-Cretaceous grains (Fig. 12; Appendix A). The Paleozoic grain is dark in CL with oscillatory zoning, elongate (≥3:1 aspect ratio), and has a LA-ICPMS date of 386 Ma. The three mid-Cretaceous grains are stubby (≤2:1 aspect ratio) and rounded with moderate brightness, sector zoning, and have LA-ICPMS dates between 108 and 99 Ma. The Late Cretaceous population of grains display dark to moderate brightness in CL, are elongate (≥3:1 aspect ratio) with sharp crystal faces, and have LA-ICPMS dates between 74.5 and 59.1 Ma. The Paleozoic to Mesozoic and mid-Cretaceous grains are interpreted to be inherited, whereas the Late Cretaceous grains are interpreted as volcanic in origin. The weighted mean age of 20 Late Cretaceous LA-ICPMS analyses is 68.9 ± 0.8 Ma; the oldest four Late Cretaceous grains are interpreted to be antecrysts, and the youngest eight grains are believed to have undergone minor Pb-loss. Six zircon grains analyzed by CA-TIMS yield concordant $^{206}Pb/^{238}U$ dates that range from 69.799 ± 0.050 to 69.739 ± 0.050 Ma (Table 1), all six grains have a weighted mean age of 69.779 ± 0.020 Ma (MSWD = 0.7, probability of fit = 0.62, n = 6/6). The weighted mean age of 69.779 ± 0.020 Ma is interpreted as the crystallization age of this sample.

Whole-rock geochemistry

Major and trace element compositions for the 27 samples are in Appendix B. Loss on ignition (LOI) for the samples are mostly between <1 to 10%. The Sixtymile district samples are mostly intermediate in composition with calc-alkaline to high potassium (K) calc-alkaline affinity (Fig. 13). The samples have between 66 and 49 wt% SiO_2, 18.1 and 14.2 wt% Al_2O_3, 3.8 to 0.4 wt% K_2O, ≤6.0 wt% Na_2O, and TiO_2 between 1.0 and 0.3 wt%. Field and petrographic observations in conjunction with the low to moderate

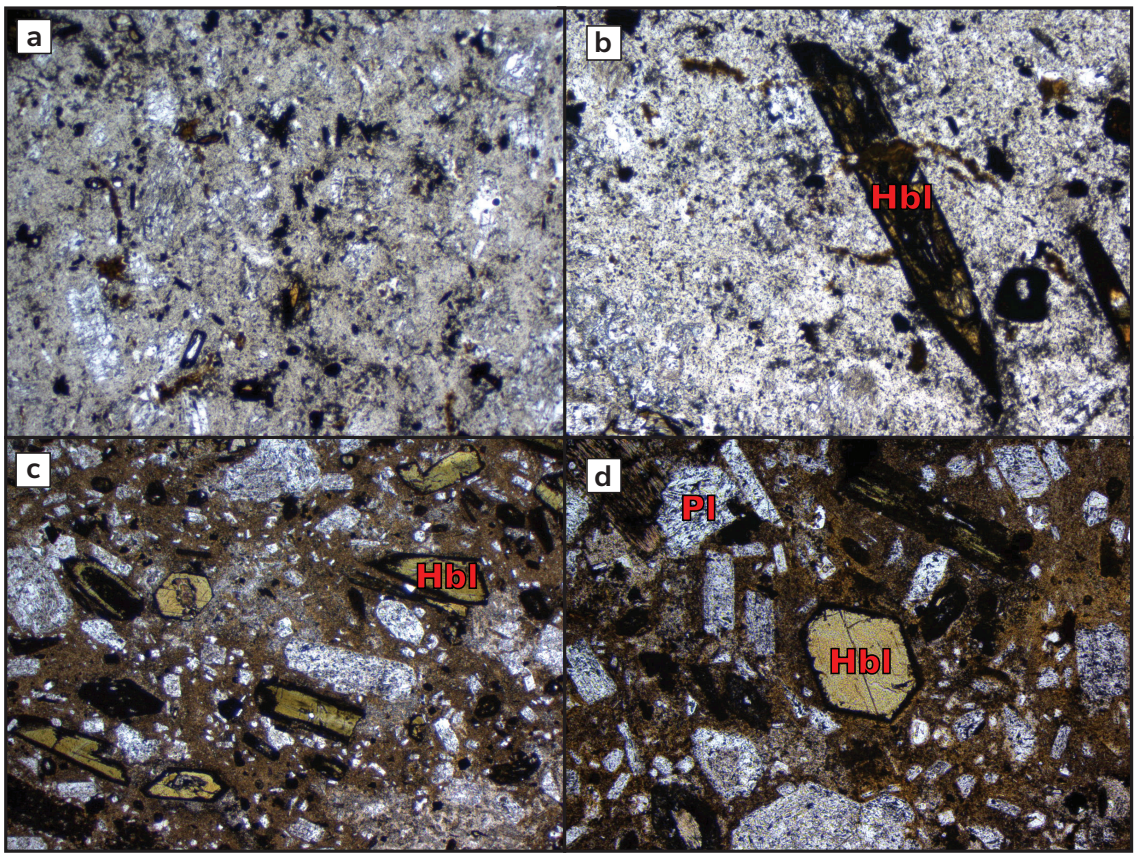

Figure 9. *Thin sections of the geochronology samples:* **(a)** *23PS004-2 in PPL at 2.5x magnification (field of view (fov) 10 mm across);* **(b)** *23PS004-2 in PPL at 5x magnification (fov 5 mm across);* **(c)** *23PS064-1 in PPL at 2.5x magnification (fov 10 mm across); and* **(d)** *23PS064-1 in PPL at 5x magnification (fov 5 mm across). Mineral abbreviations from Whitney and Evans (2010); Hbl – hornblende; Pl – plagioclase.*

LOI values, as well as scattered data on mobile element diagrams (e.g., Fig. 13), indicate that most samples have undergone at least minor alteration. Because of the alteration, rock classifications are derived from the Zr/Ti versus Nb/Y immobile element diagram, where the samples plot mainly in the andesite to basaltic andesite fields (Fig. 13).

The high field strength elements (HFSE) are relatively immobile with values that range from 92 to 150 ppm zirconium (Zr), 6.4 to 10.7 ppm niobium (Nb), 2.6 to 7.6 ppm thorium (Th), 12.1 to 22.4 ppm yttrium (Y), 0.3 to 0.7 ppm tantalum (Ta), and 2.3 to 3.6 ppm hafnium (Hf). The large ion lithophile elements (LILE) are more enriched in the samples and have concentrations of 808 to 1765 ppm barium (Ba), 552 to 996 ppm strontium (Sr), 36.6 to 87.1 ppm rubidium (Rb), 0.58 to 25.3 ppm cesium (Cs), and 0.02 to 0.09 ppm thallium (Tl). Trace element patterns for the samples show significant variation for the light rare earth elements (LREE) and are less variable for the heavy REE (HREE). Normalized against primitive

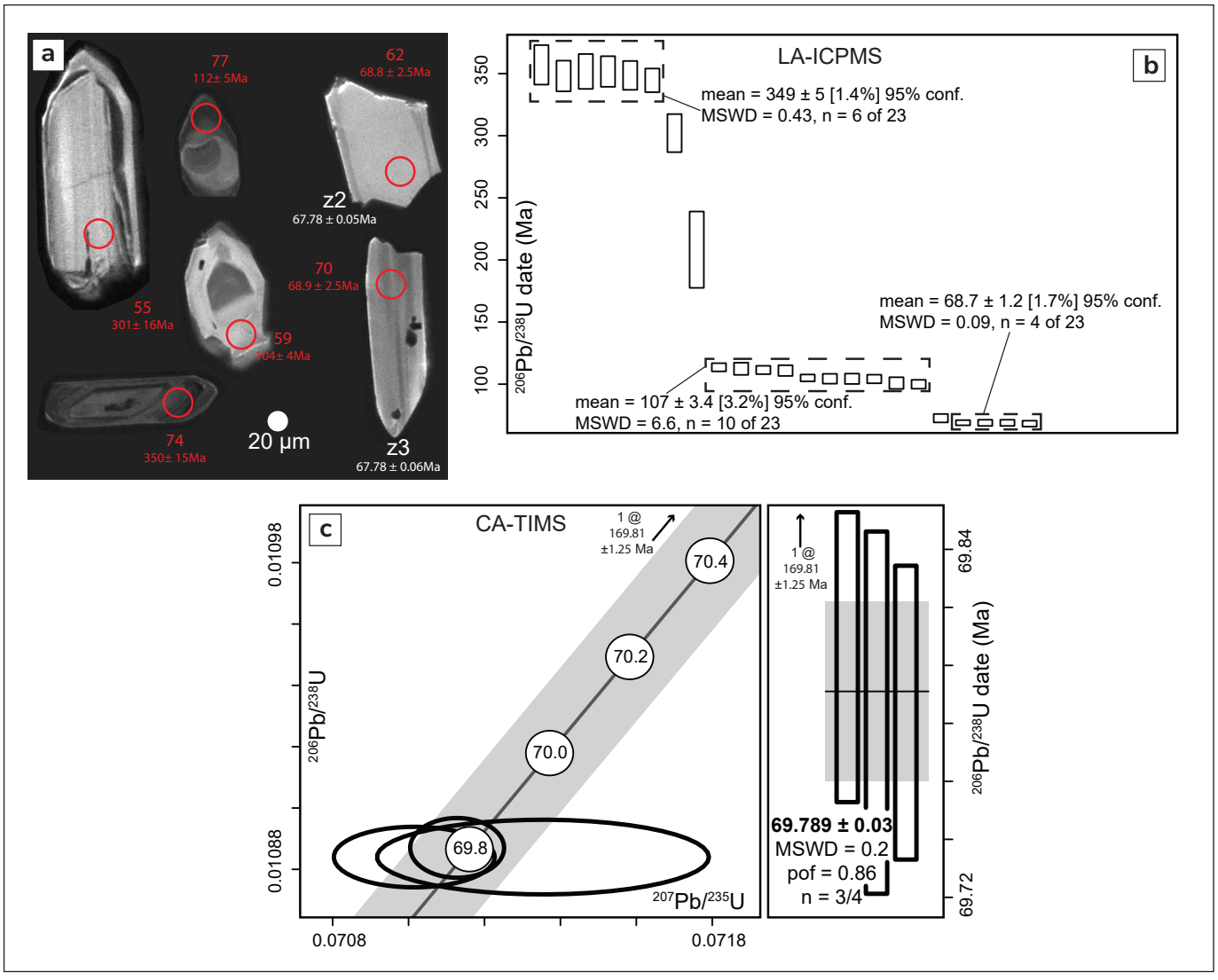

Figure 10. *Sample 23PS004-2 U-Pb geochronological results.* ***(a)*** *Cathodoluminescence images of representative igneous zircons. Red labels indicate LA-ICPMS analysis number and age with associated error; the red open circle indicates the location of the analysis spot; white analysis number and age with associated error refers to grain analyzed by CA-TIMS.* ***(b)*** *Ranked plot of LA-ICPMS $^{206}Pb/^{238}U$ dates.* ***(c)*** *Concordia diagram (left) and ranked $^{206}Pb/^{238}U$ dates (right) for zircons analyzed by CA-TIMS. Grey horizontal bar shows calculated weighted mean with error. Analyses included in weighted mean age calculations (light grey horizontal bar) are bold; analyses with thin lines are not used in calculations. The light grey band around Concordia (dark grey line) shows the decay constant uncertainties. Errors in all plots are at 2σ. MSWD – mean squared weighted deviation; pof – probability of fit; n – number of analyses included in age calculation.*

mantle values (Sun and McDonough, 1989), the LREE are enriched (La_N/Sm_N = 6.2) with moderately fractionated HREE (Gd_N/Yb_N = 2.02) and an overall negative slope (La_N/Yb_N = 9.6; Fig. 14). Barium content within all samples is high, averaging 1289 ppm with a range of 808–1765 ppm. Zirconium content for the samples has an average of 124.5 ppm, whereas Y, lanthanum (La), cerium (Ce), praseodymium (Pr), and Nd are in the tens of ppm. The trace elements do not show significant variation with increasing SiO_2. Plots of immobile REE ratios normalized to the primitive mantle display negative Ta, Nb, and Ti anomalies (e.g., Fig 14).

The Late Cretaceous volcanic rocks have $^{87}Rb/^{86}Sr$ ratios between 0.1529 and 0.3392, initial $^{87}Sr/^{86}Sr$ values ranging between 0.7050 and 0.70555, $^{143}Nd/^{144}Nd_i$ values ranging between 0.51244 and 0.5126, and εNd_i values of -1.9 to 1.1 (Table 2; Fig. 15). The values for the samples are 19.35 to 19.50 for $^{206}Pb/^{204}Pb$, 15.63 to 15.66 for $^{207}Pb/^{204}Pb$, 39.02 to 39.07 for $^{208}Pb/^{204}Pb$, 0.035 to 0.8080 for $^{207}Pb/^{206}Pb$, and 2.0095 to 2.0162 for $^{208}Pb/^{206}Pb$.

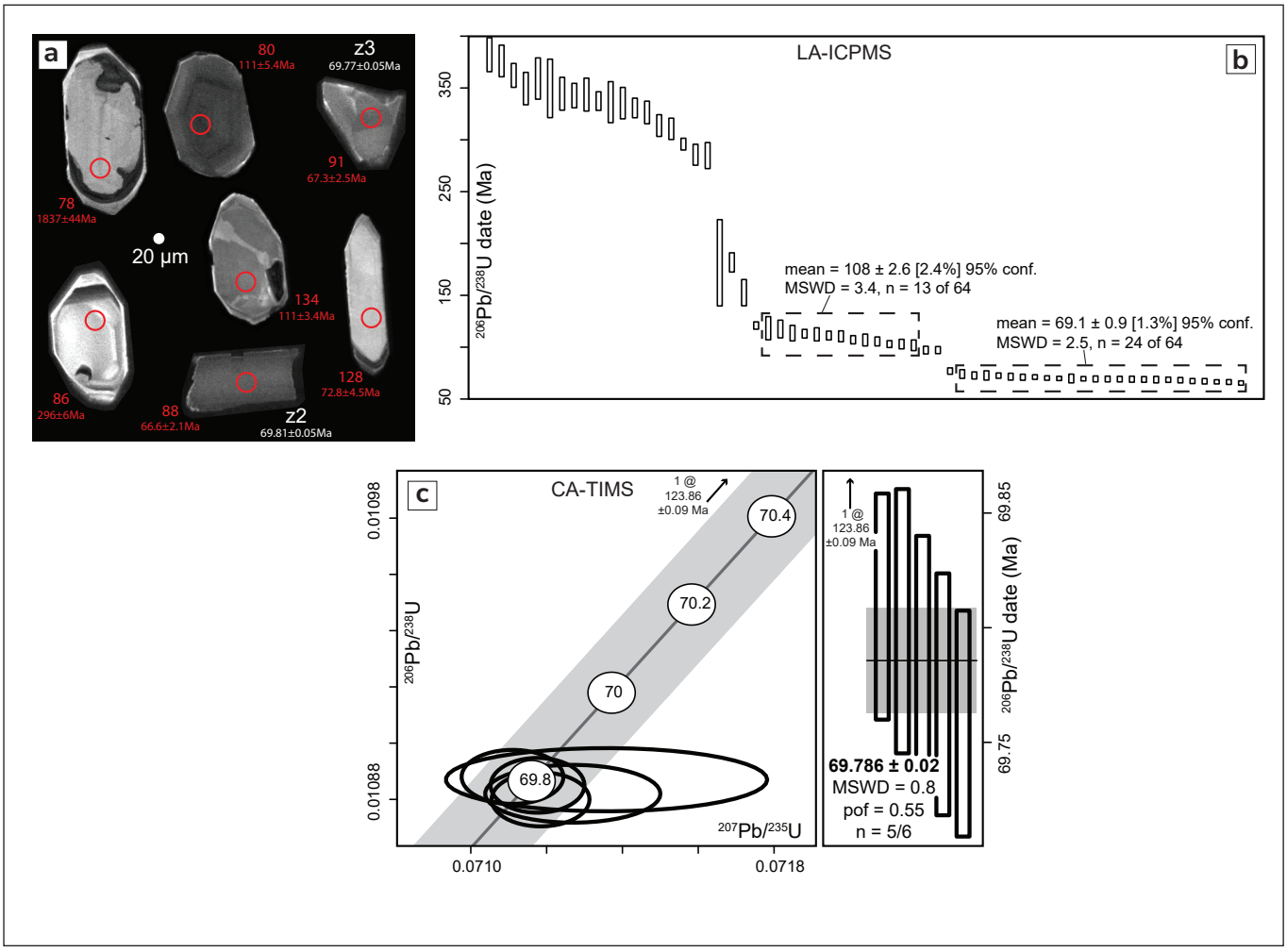

Figure 11. *Sample 23PS064-1 U-Pb geochronological results.* ***(a)*** *Cathodoluminescence images of representative igneous zircons. Red labels indicate LA-ICPMS analysis number and age with associated error; the red open circle indicates the location of the analysis spot; white analysis number and age with associated error refers to grain analyzed by CA-TIMS.* ***(b)*** *Ranked plot of LA-ICPMS $^{206}Pb/^{238}U$ dates.* ***(c)*** *Concordia diagram (left) and ranked $^{206}Pb/^{238}U$ dates (right) for zircons analyzed by CA-TIMS. Grey horizontal bar shows calculated weighted mean with error. Analyses included in weighted mean age calculations (light grey horizontal bar) are bold; analyses with thin lines are not used in calculations. The light grey band around Concordia (dark grey line) shows the decay constant uncertainties. Errors in all plots are at 2σ. MSWD – mean squared weighted deviation; pof – probability of fit; n – number of analyses included in age calculation.*

Table 2. Radiogenic isotope data for Late Cretaceous volcanic rocks in the Sixtymile district.

Sample	23PS040-1	23PS006-1	23PS028-1	23PS031-1	23PS043-1	23PS010-1
Lithology	basaltic andesite	basalt	basaltic andesite	basaltic andesite	basaltic andesite	basalt
Latitude	64.10336	64.11686	64.04378	64.08274	64.11453	64.11441
Longitude	-140.78421	-140.69200	-140.68574	-140.76922	-140.65775	-140.74912
Rb (ppm)	43.5	58.4	58.4	87.1	77.3	63.6
Sr (ppm)	822	714	552	742	834	562
$^{87}Sr/^{86}Sr$	0.7051	0.7058	0.7057	0.7056	0.7053	0.7059
2σ	0.000016	0.000006	0.000010	0.000019	0.000016	0.000021
$^{87}Rb/^{86}Sr$	0.1529	0.2364	0.3058	0.3392	0.2679	0.3271
$^{87}Sr/^{86}Sr_i$	0.70500	0.70555	0.70543	0.70527	0.70503	0.70555
Nd (ppm)	8.05	17.8	17.3	19.7	26	21.6
Sm (ppm)	4.46	4.58	3.2	4.16	5.74	5.06
$^{143}Nd/^{144}Nd$	0.5127	0.5125	0.5126	0.5126	0.5126	0.5127
2σ	0.0000053	0.0000059	0.0000067	0.0000069	0.0000059	0.0000049
$^{147}Sm/^{144}Nd$	0.3351	0.1556	0.1119	0.1277	0.1335	0.1417
$^{143}Nd/^{144}Nd_i$	0.5125	0.5124	0.5126	0.5126	0.5125	0.5126
εNd_i	-0.0358	-1.9210	0.9575	0.5096	-0.1040	1.1440
Pb (ppm)	12	6	12	10	10	6
$^{206}Pb/^{204}Pb_{corr}$	19.40	19.50	19.36	19.35	19.41	19.44
2σ	0.006	0.006	0.006	0.006	0.006	0.006
$^{207}Pb/^{204}Pb_{corr}$	15.63	15.66	15.64	15.64	15.64	15.63
2σ	0.005	0.005	0.005	0.005	0.005	0.005
$^{208}Pb/^{204}Pb_{corr}$	39.02	39.22	39.02	39.02	39.07	39.06
2σ	0.023	0.024	0.023	0.023	0.023	0.023
$^{207}Pb/^{206}Pb_{corr}$	0.81	0.80	0.81	0.81	0.81	0.80
$^{208}Pb/^{206}Pb_{corr}$	2.01	2.01	2.02	2.02	2.01	2.01

Discussion

Field relationships

The unfoliated sedimentary and volcanic rocks in the Sixtymile district form a relatively consistent stratigraphy with basal sedimentary rocks above a regional unconformity. In the main part of the graben, the sedimentary rocks appear to be conformably overlain by the andesitic unit. However, in the few instances where the basal sedimentary rocks are seen outside the graben, such as along the road to Miller Creek, as well as on the floors of old gravel pits along the Top of the World Highway, the andesitic unit is not present, and basaltic andesite directly overlies the sedimentary rocks. The age of the 'sub-Carmacks' sedimentary rocks has not been directly constrained in the Sixtymile district, and we note a lack of volcanic clasts in the conglomerate. On the lower Sixtymile River, sedimentary rocks that have a Masstrichtian fossil plant assemblage are interbedded with andesitic volcanic rocks (Lowey, 1984; 72–66 Ma, Late Cretaceous). At the time of

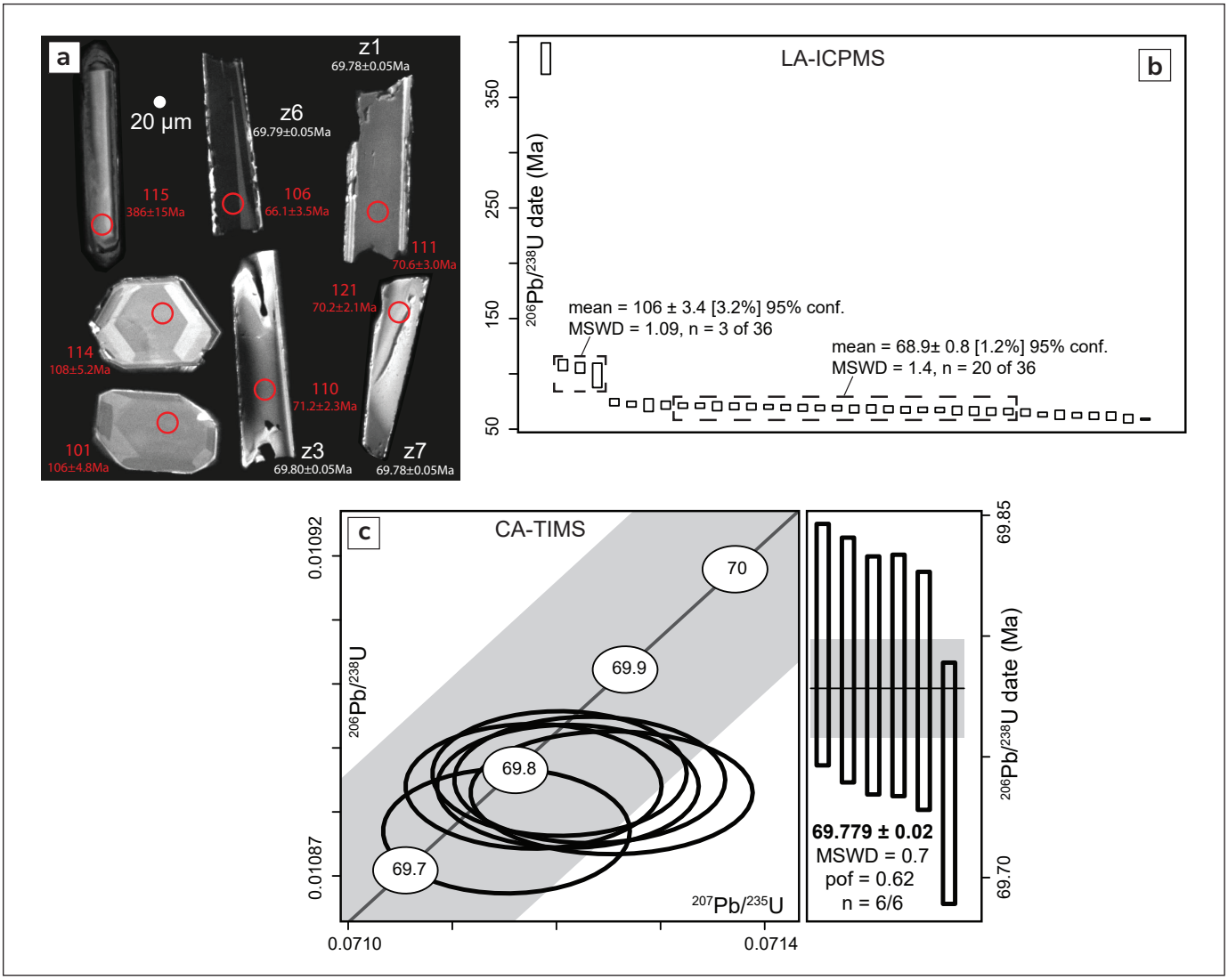

Figure 12. *Sample 23PS074-1 U-Pb geochronological results.* ***(a)*** *Cathodoluminescence images of representative igneous zircons. Red labels indicate LA-ICPMS analysis number and age with associated error; the red open circle indicates the location of the analysis spot; white analysis number and age with associated error refers to grain analyzed by CA-TIMS.* ***(b)*** *Ranked plot of LA-ICPMS* $^{206}Pb/^{238}U$ *dates.* ***(c)*** *Concordia diagram (left) and ranked* $^{206}Pb/^{238}U$ *dates (right) for zircons analyzed by CA-TIMS. Grey horizontal bar shows calculated weighted mean with error. Analyses included in weighted mean age calculations (light grey horizontal bar) are bold; analyses with thin lines are not used in calculations. The light grey band around Concordia (dark grey line) shows the decay constant uncertainties. Errors in all plots are at 2σ. MSWD – mean squared weighted deviation; pof – probability of fit; n – number of analyses included in age calculation.*

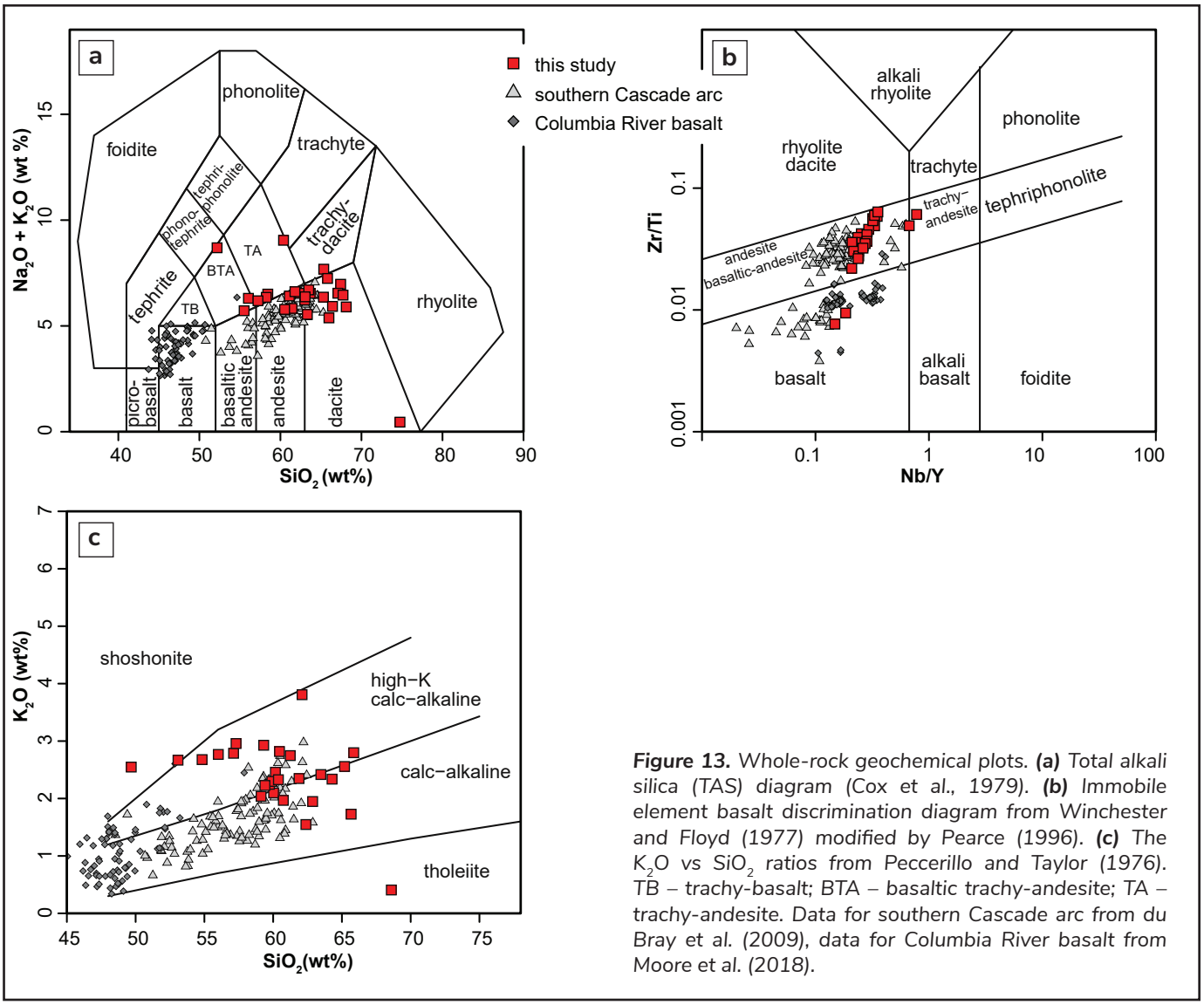

Figure 13. *Whole-rock geochemical plots.* ***(a)*** *Total alkali silica (TAS) diagram (Cox et al., 1979).* ***(b)*** *Immobile element basalt discrimination diagram from Winchester and Floyd (1977) modified by Pearce (1996).* ***(c)*** *The K_2O vs SiO_2 ratios from Peccerillo and Taylor (1976). TB – trachy-basalt; BTA – basaltic trachy-andesite; TA – trachy-andesite. Data for southern Cascade arc from du Bray et al. (2009), data for Columbia River basalt from Moore et al. (2018).*

writing, a sample of quartz-phyric tuff interbedded with the conglomerate unit was being analyzed for U-Pb zircon dating. If successful, this sample would constrain the depositional age for the sedimentary rocks.

Locally, the thickness of the sedimentary rocks is difficult to constrain precisely, but outside of the graben, such as on the road to Miller Creek, the bottom and top are discernible by colour changes in ditch material and suggest a true thickness of less than 20 m. The thickest part appears to be within the graben north of the Top of the World Highway, where there is at least 100 m of elevation change from the upper contact with the andesitic unit to where the unit truncates against a normal fault. The bottom of the sedimentary unit in contact with the metamorphic basement is not exposed in this area. Lowey (1984) estimated the thickness of the Late Cretaceous sedimentary rocks on the Lower Sixtymile River to be 200 m.

The volcanic rocks in the Sixtymile district are a mixture of relatively vent proximal facies, including block and ash flow, autoclastic breccia and massive, coherent flows with subordinate distal facies such as ash (tuff) deposits. The volcanic rocks appear to be part of the same magmatic cycle, as indicated by their similar immobile chemistry (see below) and a gradational mafic phenocryst assemblage. The basal andesite is hornblende-bearing throughout, but is biotite-bearing in its lower sections, and pyroxene-bearing in its upper sections as it transitions to a basaltic andesite; the basaltic

andesite has pyroxene ± olivine phenocrysts. The contact between the andesite and basaltic andesite on our map is inferred to be a transitional contact, not a sharp contact. We interpret these rocks to be from a single magmatic cycle having slightly more evolved compositions at the start that get increasingly juvenile as the cycle progresses.

Geochronology

Our four new U-Pb zircon CA-TIMS ages from throughout the andesitic component of the stratigraphy all overlap within error, indicating that these rocks erupted in less than 60 ka (total age range of 69.822 to 69.763 ka including internal errors). This tightly constrains the age of the volcanic event in the Sixtymile district to ca. 69.8 Ma. The age of the upper basaltic andesite unit is not directly constrained, except in that it is younger than the andesitic part of the stratigraphy. Plutonism in a slightly larger area around the Sixtymile district, and where constrained by high precision CA-TIMS U-Pb zircon ages, is less than one million years younger than volcanism (Fig. 15). This is consistent with observations of plutonic rocks crosscutting volcanic rocks within the study area, and emphasizes that the overall magmatic event was still short in duration (<1 m.y.).

All four samples analyzed for U-Pb zircon had inherited Paleozoic to Mesozoic grains (plus one sample with a Paleoproterozoic grain) and mid-Cretaceous grains. The Paleozoic grains are predominantly euhedral, elongate and match local units well, and include Devonian to Mississippian populations (Finlayson Assemblage), Permian grains (Klondike Assemblage), and a few Jurassic grains (Minto suite). The mid-Cretaceous grains differ in that they are generally stubby and rounded. Although a few scattered intrusions of this age occur to the south, there are not many local sources for mid-Cretaceous zircons. One possibility is that these mid-Cretaceous grains are sourced from the underlying sedimentary unit. This could imply the sediment source for those rocks was to the south where there are mapped mid-Cretaceous

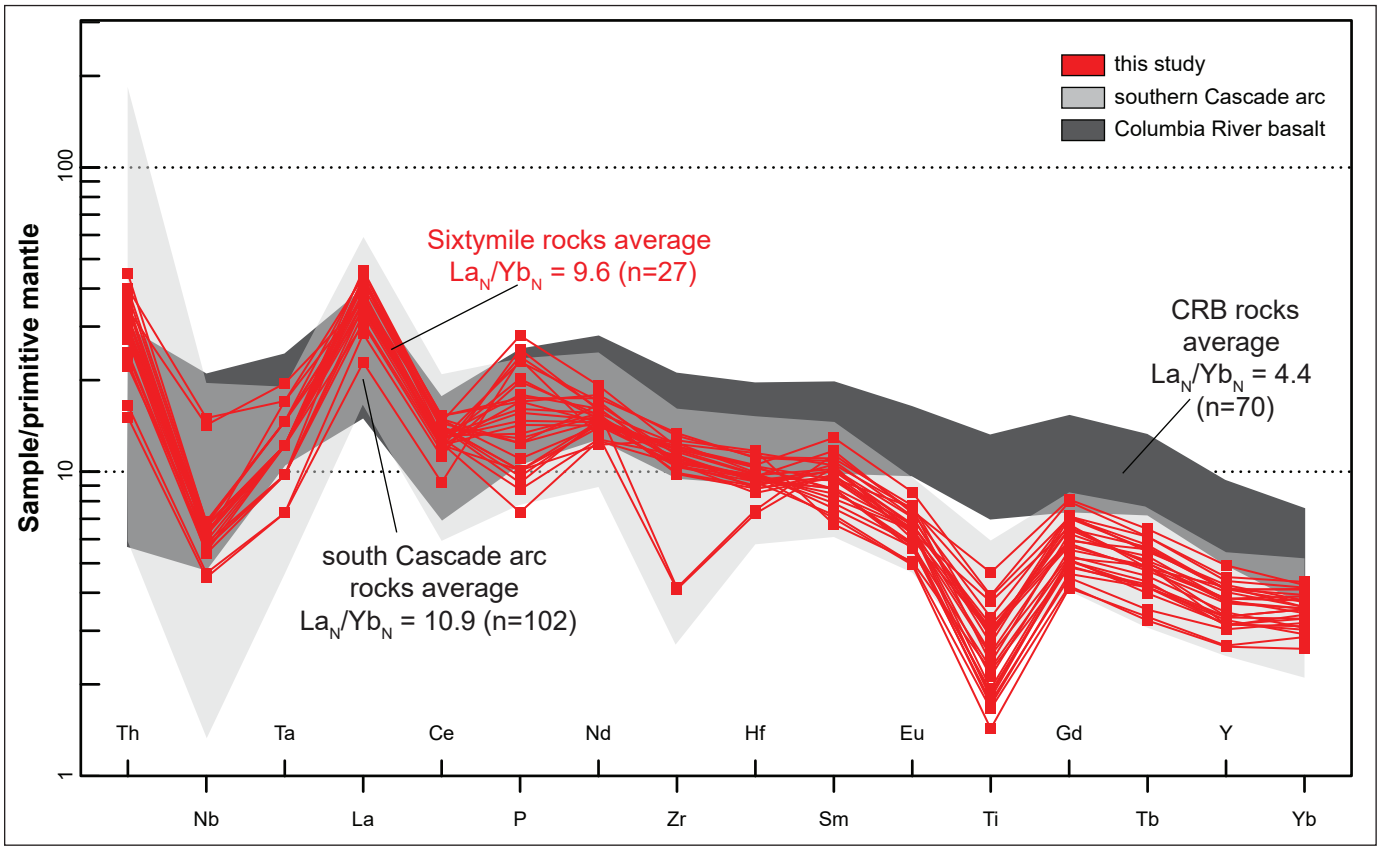

Figure 14. *Immobile rare earth element (REE) spider plot normalized to primitive mantle (Sun and McDonough, 1989). Symbols and data same as Figure 13.*

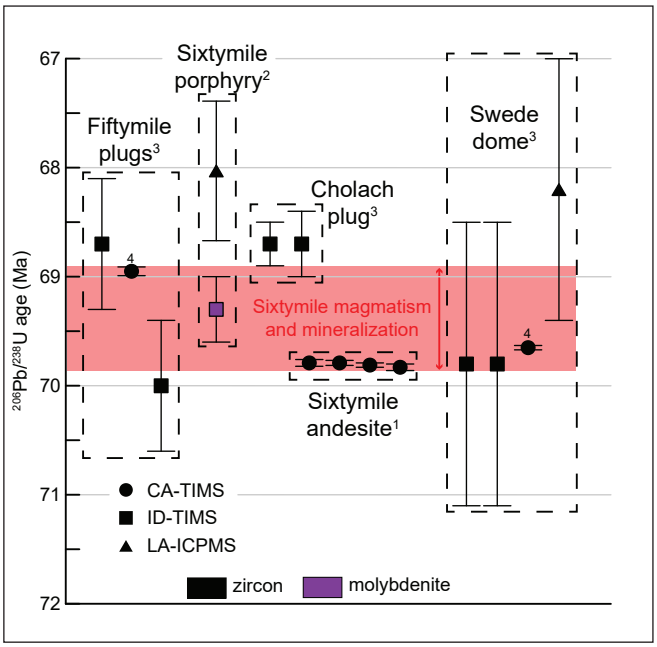

Figure 15. *Summary of Late Cretaceous geochronological data for the Sixtymile area. Superscripts: 1 – this study; 2 – Allen et al. (2017); 3 – Mortensen (Yukon Geological Survey, 2023); and 4 – Sack (Yukon Geological Survey, 2023).*

intrusions within the Fiftymile batholith. The latter interpretation would be consistent with Lowey (1984), who suggested a southern sedimentary source and noted rare kyanite in the sandy matrix of conglomerate units, potentially sourced from the autochthonous North American rocks in that region (e.g. Dusel-Bacon et al., 2002). However, we note that there are scattered mid-Cretaceous plutons to the north and east as well.

Geochemistry

Assessment of alteration

The iron oxides visible in thin section suggest the samples are weakly weathered. The minor carbonate and clay that replaces plagioclase and amphibole phenocrysts may be evidence of a CO_2-rich fluid interacting with the volcanic rocks (e.g., Wynne et al., 1998). Low to moderate loss on ignition values and the observations above suggest the rocks have undergone minor alteration (Appendix B), but when comparing the total-alkali-silica (TAS) diagram (Le Bas et al., 1986) or K_2O versus SiO_2 (Peccerillo and Taylor, 1976) with the Nb/Y versus Zr/Ti diagram (Pearce, 1996), the mobile element (e.g., SiO_2, Na_2O, K_2O) classifications are slightly more felsic and alkalic suggesting some element mobility. The andesitic and basaltic andesite classification used here is based on petrography and the Nb/Y versus Zr/Ti diagram of Pearce (1996). Because of the apparent element mobility, we mostly restrict our geochemical interpretations to those based on immobile elements.

Tectonic setting

The andesitic and basaltic andesite samples are very similar geochemically (Figs. 13 to 16). Based on the similar geochemistry and the phenocryst assemblage discussed above, we interpret these rocks to be part of the same magmatic event and thus genetically related. Despite possible mobility of some elements, major element geochemical compositions for all the rocks in this study straddle the calc-alkaline and high-K calc-alkaline fields of Peccerillo and Taylor (1976). Continental crust is geochemically modelled as intermediate in composition and contains elevated incompatible trace elements such as Th and Nb relative to Yb (Rudnick, 1995). The high values of both Th/Yb (>1) and Nb/Yb (3–10) are consistent with recycled material incorporated from the crust. This can be seen on various geochemical discrimination diagrams where our samples plot in the calc-alkaline compressional arc field (Fig. 16a), the volcanic arc field (Fig. 16b), the continental arc basalt (CAB) field (Fig. 16c), and to the bottom right of the volcanic arc discrimination line, in a field characteristic of continental arcs (Fig. 16d).

The Late Cretaceous volcanic rocks are depleted in HFSE and LREE relative to LILE, a pattern consistent with an arc setting (Basta et al., 2017). The immobility and low solubility of HFSE relative to LILE causes different melting behaviours during subduction (Zack et al., 2002). As a down-going slab dehydrates, it releases fluids with mobile LILE, but the immobile HFSE remain in the slab. This decoupling leads to their respective enrichment and depletion as evident in Figure 14. Trace element diagrams normalized to primitive mantle reveal distinct volcanic arc chemical signatures such as negative Nb, Ta and Ti anomalies (Fig. 14). The negative Ta-Nb trough anomaly is typical for volcanic arc settings and is consistent with crustal contamination (Xia, 2014). The trace element geochemistry suggests crustal contamination was involved in the formation of the Late Cretaceous volcanic rocks in the Sixtymile district.

Supporting evidence for a continental arc setting comes from Sr-Nd-Pb radiogenic isotopes. Magmas

that have interacted with crustal rocks are more abundant in Rb compared to primitive magmas (Rollinson et al., 2021) a pattern evident in our dataset. The Rb/Sr values for oceanic basalts are less than 0.1 and magmas derived entirely from continental crust can be up to 2.0 (Rollinson et al., 2021). The Sixtymile district samples $^{87}Rb/^{86}Sr$ (0.1529–0.3392) values are indicative of juvenile magma that interacted with continental crust. In the mantle source diagram ($^{87}Sr/^{86}Sr$ versus $^{143}Nd/^{144}Nd$) the samples plot just below bulk earth (BE) in the enriched mantle (EM1) field, suggesting an enriched mantle source (Rollinson et al., 2021). Additionally, positive εNd_i values are consistent with depleted mantle reservoirs and negative εNd_i values are consistent with an enriched mantle or crustal source (Allègre and Rousseau, 1984). Magmas that have interacted with crustal rocks have more evolved Pb isotope ratios as lead is sensitive to crustal processes and is highly concentrated in the crust. The elevated Pb isotopes in our data set are higher than the values typical for MORB or OIB, suggesting the magma has interacted with continentally derived rocks, such as rocks from the Yukon Tanana basement (Fig. 17).

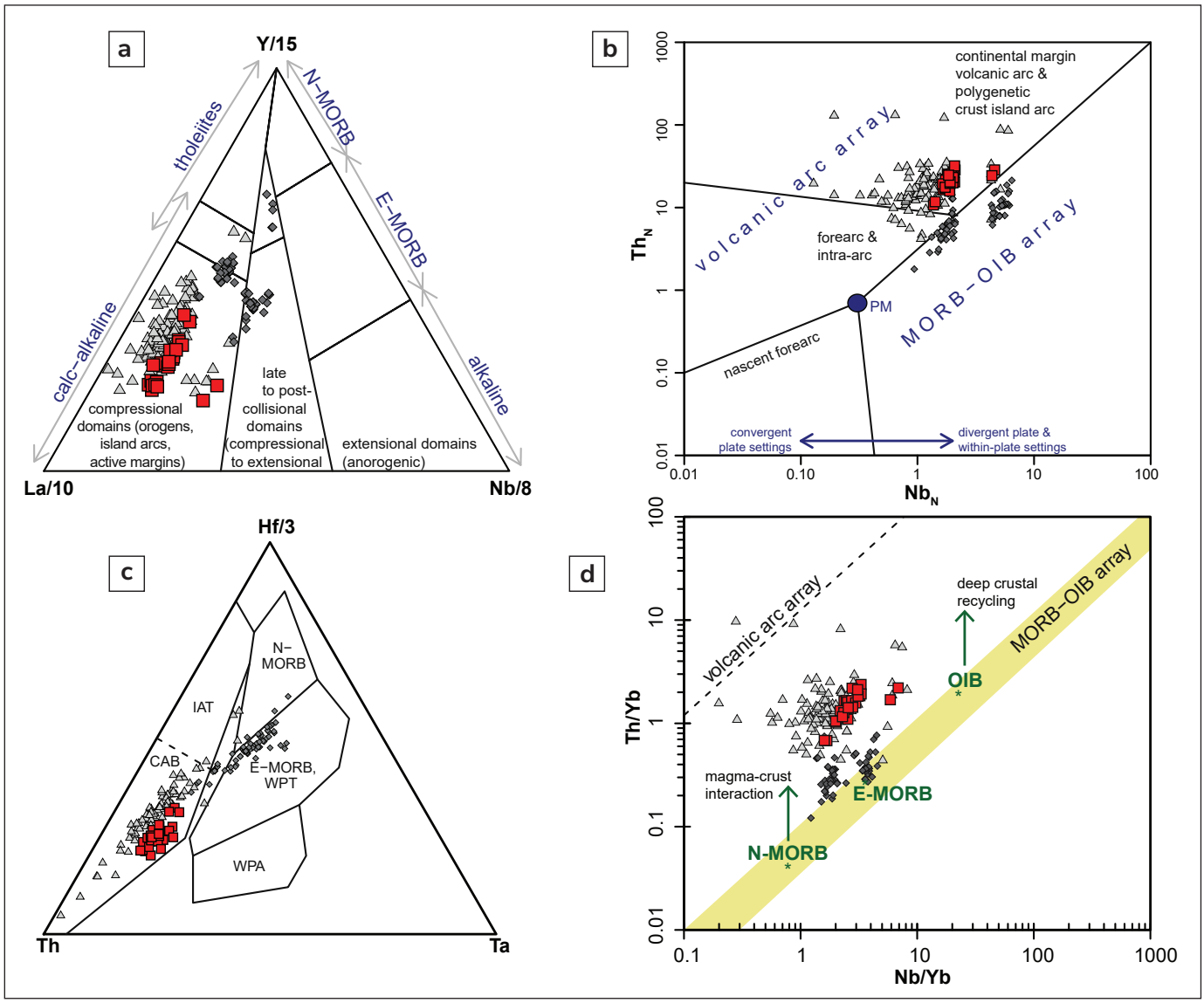

Figure 16. *Geochemical tectonic setting discrimination diagrams.* ***(a)*** *Crustal mixing or contamination (Cabanis and Lecolle, 1989).* ***(b)*** *Tectonic setting (Saccani, 2015).* ***(c)*** *Tectonic setting (Wood, 1980).* ***(d)*** *Basalt Th/Yb versus Nb/Yb diagram (Pearce, 2008). MORB – mid-ocean ridge basalt; N – normal; E – enriched; OIB – ocean island basalt; CAB – continental arc basalt; IAT – island arc tholeiite; WPT – within-plate tholeiite; and WPA – within-plate alkalic. Symbols and data same as Figure 13.*

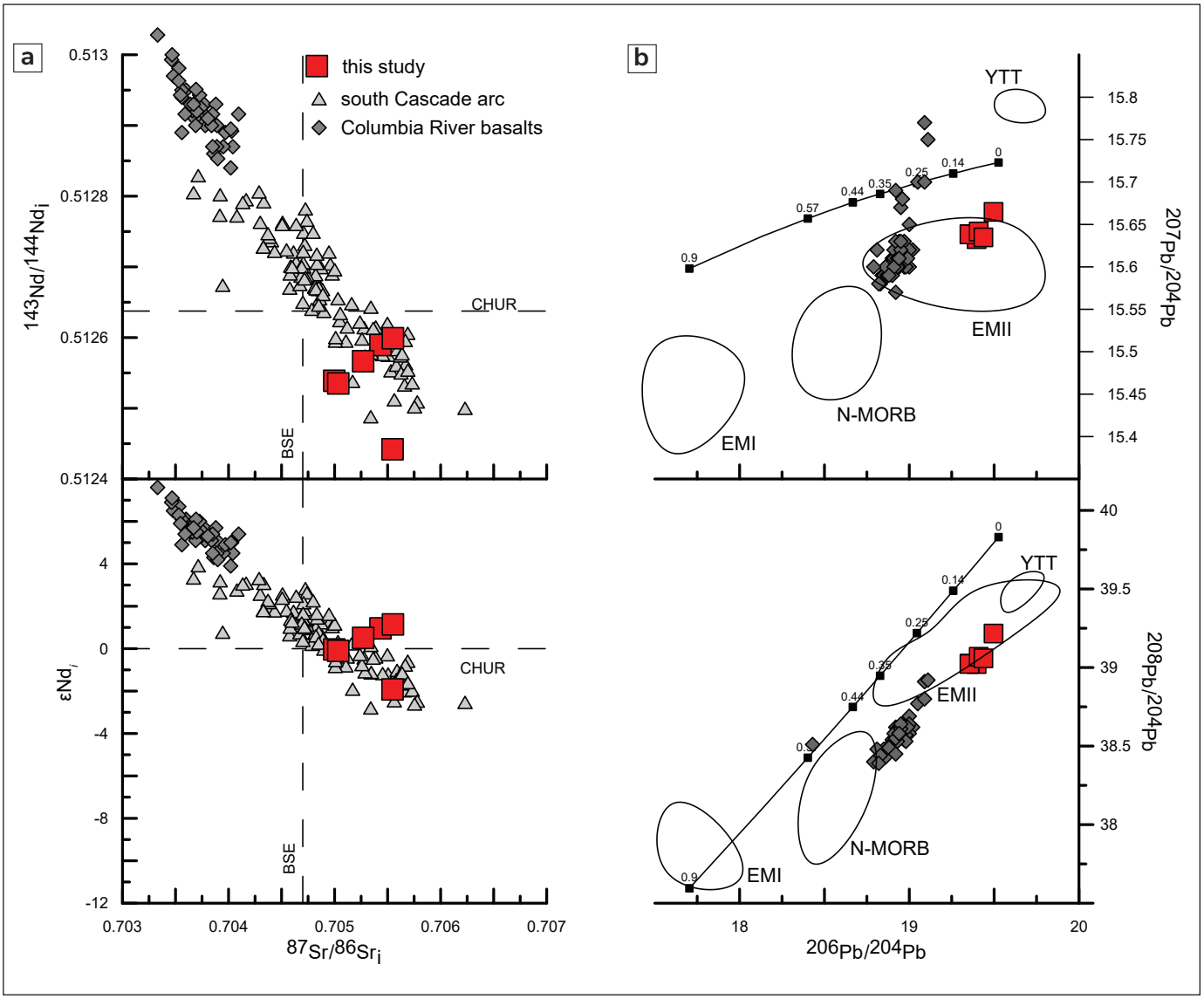

Figure 17. *Whole-rock isotope plots for Sixtymile volcanic rocks.* **(a)** *Initial Nd and εNd_i vs. initial Sr. Data for southern Cascade arc from du Bray et al. (2009), and data for Columbia River basalt from Moore et al. (2020). BSE – bulk silicate Earth; CHUR – chondritic uniform reservoir.* **(b)** *Plot of ^{207}Pb and ^{208}Pb vs ^{206}Pb. Data for enriched mantle I (EMI), enriched mantle II (EMII) and ocean island basalt (OIB) fields from Hart (1988); normal-mid ocean ridge basalt (N-MORB) from Ito et al. (1987); and Columbia River basalt from Moore et al. (2020). Yukon Tanana terrane (YTT) fields are based on samples of Sulphur Creek suite and Snowcap assemblage with data from Selby et al. (1999). Shale curve from Godwin and Sinclair (1982) and appears valid for parautochthonous terranes (Mortensen et al., 2006); ages in Ga.*

Summary

Late Cretaceous magmatic rocks across the northern Cordillera include small, high-level, calc-alkaline felsic to intermediate plutons (e.g., Friend, 2022) that are broadly coeval, and possibly comagmatic, with more widespread subaerial intermediate to mafic volcanic rocks of the Carmacks group (Grond et al., 1984; Woodsworth et al., 1991; Johnston et al., 1996). The volcanic rocks display calc-alkaline trace element signatures, but the high MgO contents of the mafic rocks have been interpreted as evidence of a mantle source (Johnston et al., 1996; Francis and Minarik, 2008). A few possible tectonic settings have been suggested based on these characteristics, including magmatism associated with oblique east-dipping subduction (Souther, 1991), a mantle plume source (Johnston et al., 1996), and subduction-related magmatism followed by slab rupture (Friend, 2022).

In the Sixtymile district, the lower part of the Late Cretaceous rocks appear to be exposed. The basal conglomerate unit in contact with the metamorphic basement is clearly observed, and the overlying rocks are dominantly andesitic, transitioning to basaltic andesite in the uppermost parts of the preserved volcanic stratigraphy. The new U-Pb zircon and CA-TIMS ages obtained from the andesitic component of the stratigraphy constrain the volcanic event in the Sixtymile district to approximately 69.8 Ma. Though the other areas with Late Cretaceous volcanic rocks are not as well constrained geochronologically, it is generally thought that the upper, basaltic component is ca. 72 to 69 Ma (Grond et al., 1984; Lowey et al., 1986). Elsewhere in the Yukon, Late Cretaceous, intermediate calc-alkaline volcanic rocks are considerably older, e.g., Tlansanlin (Morris et al., 2014) and Open Creek (Bordet et al., 2019) rocks in southern Yukon, which are ca. 79 to 76 Ma.

Geochemical data and phenocryst assemblages throughout the volcanic sequence indicate that the andesitic and basaltic andesite units were generated by a single, genetically related magmatic event. Major and trace element patterns (high Th/Yb and Nb/Yb values, negative Nb-Ta-Ti anomalies) and radiogenic Sr-Nd-Pb isotopes support a subduction setting with crustal contamination. These results differ from interpretations of Carmacks volcanic rocks having a mantle plume source (Johnston et al., 1996), characterized by shoshonitic magnesium-rich lavas and alkaline signatures. Instead, the Sixtymile district rocks lack these alkaline signatures and are more typical of young, primitive continental arc magmatism, supporting a subduction-related origin (e.g., Friend, 2022).

Conclusions

The geologic mapping, U-Pb zircon geochronology, whole-rock geochemistry, and Sr-Nd-Pb isotopic analyses presented in this study refine the understanding of Late Cretaceous volcanic rocks in the Sixtymile district. We suggest the Sixtymile volcanic sequence represents part of a Late Cretaceous continental magmatic arc system based on the following data:

1. Bedrock geology consists of a Yukon-Tanana terrane metamorphic basement overlain by relatively undeformed and unmetamorphosed Cretaceous sedimentary and volcanic rocks. The Cretaceous rocks have a consistent stratigraphy including a sedimentary basal unit, an andesitic middle unit, and a basaltic andesite upper unit.

2. Four new U-Pb zircon CA-TIMS ages from the andesitic component tightly constrain the volcanic event to ca. 69.8 Ma.

3. Whole-rock geochemical data indicate the volcanic rocks are dominantly sub-alkaline with continental arc geochemical signatures: (a) Th/Yb versus Nb/Yb ratios plot within the volcanic arc field; (b) extended trace element patterns reveal negative Nb-Ta anomalies and positive Pb anomalies; and (c) HFSE and LREE are depleted compared to LILE.

4. Isotopic values of $^{87}Rb/^{86}Sr$ (0.1529 - 0.3392), $^{143}Nd/^{144}Nd_i$ (0.51244 to 0.5126; εNd values of -1.9 to 1.1), and relatively enriched $^{206}Pb/^{204}Pb$ (19.35 to 19.50), $^{207}Pb/^{204}Pb$ (15.63 to 15.66), $^{208}Pb/^{204}Pb$ (39.02 to 39.07) suggest juvenile magma interaction with continental crust, consistent with a continental arc setting.

Acknowledgments

The authors would like to thank Mike MacDougall, Jayce Murtagh, John Flynn, Laurie Downes and other placer operators for access, advice on where to camp, and generally welcoming us to the Sixtymile area. Jim Ryan, Jan Dettmer and Jim Mortensen provided constructive criticism on earlier drafts of this manuscript.

References

Allan, M.A., Mortensen, J.K., Hart, C.J.R., Bailey, L.A., Sanchez, M.G., Ciolkiewicz, W., McKenzie, G.G. and Creaser, R.A., 2013. Magmatic and metallogenic framework of west-central Yukon and eastern Alaska. In: Tectonics, Metallogeny and discovery: The North American Cordillera and similar accretionary setttings, M. Colpron, T. Bissig, B.G. Rusk and J.F.H. Thompson (eds.), Society of Economic Geologists, p. 111–168.

Allan, M.M., Mortensen, J., Sanchez, M.G. and Hart, C.J.R., 2017. Structural and geochronological controls on Late Cretaceous porphyry and epithermal mineralization of the orogen-transverse Sixtymile-Pika fault system, Yukon and Alaska. Internal unpublished report, Mineral Deposits Research Unit, Vancouver, BC, 34 p.

Allègre, C.J. and Rousseau, D., 1984. The growth of the continent through geological time studied by Nd isotope analysis of shales. Earth and Planetary Science Letters, vol. 67, no. 1, p. 19–34.

Basta, F.F., Maurice, A.E., Bakhit, B.R., Azer, M.K. and El-Sobky, A.F., 2017. Intrusive rocks of the Wadi Hamad area, northeastern Desert, Egypt: Change of magma composition with maturity of Neoproterozoic continental island arc and the role of collisional plutonism in the differentiation of arc crust. Lithos, vol. 288, p. 248–263.

Bordet, E., Crowley, J.L. and Piercey, S.J., 2019. Geology of the eastern Lake Laberge area (105E), south-central Yukon. Yukon Geological Survey, Open File 2019-1, 120 p.

Cabanis, B. and Lecolle, M., 1989. Le diagramme La/10-Y/15-Nb/8; un outil pour la discrimination des series volcaniques et la mise en evidence des processus de melange et/ou de contamination crustale. The La/10-Y/15-Nb/8 diagram; a tool for distinguishing volcanic series and discovering crustal mixing and/or contamination. Comptes Rendus de l'Academie des Sciences, Serie 2: Mecanique, Physique, Chimie, Sciences de l'Univers, Sciences de la Terre, vol. 309, no. 20, p. 2023–2029.

Colpron, M., McClelland, W.C., Piercey, S.J., Kroeger, E.D.L., Crowley, J.L. and Gehrels, G.E., 2025. Revisiting the “Klondike Orogeny”: Permian to Jurassic development of the Yukon-Tanana terrane, northern Canadian Cordillera. Tectonics, vol. 44, no. 6, e2024TC008748, https://doi.org/10.1029/2024TC008748.

Colpron, M., Nelson, J.L. and Murphy, D.C., 2006. A tectonostratigraphic framework for the pericratonic terranes of the northern Canadian Cordillera In: Paleozoic evolution and metallogeny of pericratonic terranes at the ancient margin of North America, Canadian and Alaskan Cordillera, M. Colpron and J.L. Nelson (eds.), Geological Association of Canada, p. 1–23.

Colpron, M., Nelson, J.L. and Murphy, D.C., 2007. Northern Cordilleran terranes and their interactions through time. GSA Today, vol. 17, no. 4/5, p. 4–10.

Colpron, M., Sack, P.J., Crowley, J.L., Beranek, L.P. and Allan, M.M., 2022. Late Triassic to Jurassic magmatic and tectonic evolution of the Intermontane terranes in Yukon, northern Canadian Cordillera: Transition from arc to syn-collisional magmatism and post-collisional lithospheric delamination. Tectonics, vol. 41, no. 2, https://doi.org/10.1029/2021TC007060.

Cox, K.G., Bell, J.D. and Pankhurst, R.J., 1979. The interpretation of igneous rocks. Allen and Unwin, London, 450 p.

Crowley, J.L., Schoene, B. and Bowring, S.A., 2007. U-Pb dating of zircon in the Bishop Tuff at the millennial scale. Geology, vol. 35, p. 1123–1126.

du Bray, E.A., John, D.A., Putirka, K. and Cousens, B.L., 2009. Geochemical database for igneous rocks of the ancestral Cascades arc—southern segment, California and Nevada. United States Geological Survey, Data Series 439, 24 p.

Duk-Rodkin, A., 1996. Surficial geology, Dawson, Yukon Territory. Geological Survey of Canada, Open File 3288, scale 1:250 000.

Dusel-Bacon, C., Hopkins, M.J., Mortensen, J.K., Dashevsky, S.S., Bressler, J.R. and Day, W.C., 2006. Paleozoic tectonic and metallogenic evolution of the pericratonic rocks of east-central Alaska and adjacent Yukon. In: Paleozoic Evolution and Metallogeny of Pericratonic Terranes at the Ancient Pacific Margin of North America, Canadian and Alaskan Cordillera, M. Colpron and J.L. Nelson (eds.), Geological Association of Canada, p. 25–74.

Dusel-Bacon, C., Lanphere, M.A., Sharp, W.D., Layer, P.W. and Hansen, V.L., 2002. Mesozoic thermal history and timing of structural events for the Yukon–Tanana Upland, east-central Alaska: 40Ar/39Ar data from metamorphic and plutonic rocks. Canadian Journal of Earth Sciences, vol. 39, no. 6, p. 1013–1051.

Dusel-Bacon, C. and Mortensen, J., 2024. New U-Pb geochronology and geochemistry of Paleozoic metaigneous rocks from western Yukon and eastern Alaska, cross-border synthesis, and implications for tectonic models. US Geological Survey Professional Paper 1888, 100 p., https://doi.org/10.3133/pp1888.

Francis, D. and Minarik, W., 2008. Aluminum-dependent trace element partitioning in clinopyroxene. Contributions to Mineralogy and Petrology, vol. 156, p. 439–451.

Friend, M., 2022. Tectonomagmatic framework for Late Cretaceous postsubduction magmatism in west-central Yukon and southern Yukon. MSc thesis, University of British Columbia, Vancouver, British Columbia, 550 p.

Garrity, C.P. and Soller, D.R., 2009. Database of the geologic map of North America— Adapted from the map by J.C. Reed, Jr. and others (2005). US Geological Survey Data Series 424, https://pubs.usgs.gov/ds/424/.

Glasmacher, U. and Friedrich, G., 1992. Volcanic-hosted epithermal gold-sulphide mineralization and associated enrichment processes, Sixtymile River area, Yukon Territory, Canada. In: Yukon Geology, Volume 3, T.J. Bremner (ed.), Exploration and Geological Services Division, Yukon Region, Indian and Northern Affairs Canada, p. 271–291.

Godwin, C.I. and Sinclair, A.J., 1982. Average lead isotope growth curves for shale-hosted zinc-lead deposits, Canadian Cordillera. Economic Geology, vol. 77, no. 3, p. 675–690.

Grond, H.C., Churchill, S.J., Armstrong, R.L., Harakal, J.E. and Nixon, G.T., 1984. Late Cretaceous age of the Hutshi, Mount Nansen, and Carmacks groups, southwestern Yukon Territory and northwestern British Columbia. Canadian Journal of Earth Sciences, vol. 21, no. 5, p. 554–558.

Hart, S.R., 1988. Heterogeneous mantle domains: signatures, genesis and mixing chronologies. Earth and Planetary Science Letters, vol. 90, no. 3, p. 273–296.

Ito, E., White, W.M. and Göpel, C., 1987. The O, Sr, Nd and Pb isotope geochemistry of MORB. Chemical Geology, vol. 62, no. 3, p. 157–176.

Jaffey, A.H., Flynn, K.F., Glendenin, L.F., Bentley, W.C. and Essling, A.M., 1971. Precision measurements of half-lives and specific activities of 235U and 238U. Physical Review C, vol. 4, no. 5, p. 1889–1906.

Johnston, S.T. and Erdmer, P., 1995. Magmatic flow and emplacement foliations in the Early Jurassic Aishihik batholith, southwest Yukon: Implications for northern Stikinia. In: Jurassic Magmatism and Tectonics of the North American Cordillera, D.M. Miller and C. Busby (eds.), Geological Society of America Special Paper, https://doi.org/10.1130/SPE299-p65.

Johnston, S.T., Wynne, P.J., Francis, D., Hart, C.J.R., Enkin, R.J. and Engebretson, D.C., 1996. Yellowstone in Yukon: The Late Cretaceous Carmacks Group. Geology, vol. 24, no. 11, p. 997–1000.

Le Bas, M.J., Le Maitre, R.W., Streckeisen, A. and Zanettin, B., 1986. A Chemical Classification of Volcanic Rocks Based on the Total Alkali-Silica Diagram. Journal of Petrology, vol. 27, p. 745–750.

Lowey, G., 1984. The stratigraphy and sedimentology of siliciclastic rocks, west-central Yukon, and their tectonic implications. PhD thesis, University of Calgary, Calgary, Alberta, 620 p.

Lowey, G.W., Sinclair, W.D. and Hills, L.V., 1986. Additional K-Ar isotopic dates for the Carmacks Group (Upper Cretaceous), west-central Yukon. Canadian Journal of Earth Sciences, vol. 23, p. 1857–1859.

Mattinson, J.M., 2005. Zircon U/Pb chemical abrasion (CA-TIMS) method; combined annealing and multi-step partial dissolution analysis for improved precision and accuracy of zircon ages. Chemical Geology, vol. 220, no. 1-2, p. 47–66.

Moore, N.E., Grunder, A.L. and Bohrson, W.A., 2018. The three-stage petrochemical evolution of the Steens Basalt (southeast Oregon, USA) compared to large igneous provinces and layered mafic intrusions. Geosphere, vol. 14, no. 6, p. 2505–2532.

Moore, N.E., Grunder, A.L., Bohrson, W.A., Carlson, R.W. and Bindeman, I.N., 2020. Changing Mantle Sources and the Effects of Crustal Passage on the Steens Basalt, SE Oregon: Chemical and Isotopic Constraints. Geochemistry, Geophysics, Geosystems, vol. 21, issue 8, https://doi.org/10.1029/2020GC008910.

Morris, G.A., Mortensen, J.K. and Israel, S., 2014. U-Pb age, whole-rock geochemistry and radiogenic isotopic compositions of Late Cretaceous volcanic rocks in the central Aishihik Lake area, Yukon (NTS 115H) In: Yukon Exploration and Geology 2013, K.E. MacFarlane, M.G. Nordling and P.J. Sack (eds.), Yukon Geological Survey, p. 133–145.

Mortensen, J.K., 1988. Geology southwestern Dawson map area, Yukon. Geological Survey of Canada, Open File 1927, scale 1:250 000.

Mortensen, J.K., 1996. Geological compilation maps of the northern Stewart River area, Klondike and Sixtymile districts (115N/15, 16, 115O/13, 14 and Parts of 115O/15, 16). Indian & Northern Affairs Canada/Department of Indian & Northern Development: Exploration & Geological Services Division, Open File 1996-1(G), 43 p.

Mortensen, J.K., Dusel-Bacon, C., Hunt, J.A. and Gabites, J., 2006. Lead isotopic constraints on the metallogeny of middle and late Paleozoic syngenetic base-metal occurrences in the Yukon-Tanana and Slide Mountain/Seventymile terranes and adjacent portions of the North American miogeocline. In: Paleozoic Evolution and Metallogeny of Pericratonic Terranes at the Ancient Pacific Margin of North America, Canadian and Alaskan Cordillera, M. Colpron and J.L. Nelson (eds.), Geological Association of Canada, p. 261–279.

Payne, J., Gonzales, R.A., Akhurst, K. and Sisson, W.G., 1987. Geology of Colorado Creek (115-J/10), Selwyn River (115-J/9) and Prospector Mountain (115-I/15) map areas. Indian and Northern Affairs, Open File 1987-3, p. 150.

Pearce, J.A., 1996. A user's guide to basalt discrimination diagrams. In: Trace element geochemistry of volcanic rocks, D.A. Wyman (ed.), Geological Association of Canada - Mineral Deposits Division, p. 79–113.

Pearce, J.A., 2008. Geochemical fingerprinting of oceanic basalts with applications to ophiolite classification and the search for Archean oceanic crust. Lithos, vol. 100, p. 14–48.

Peccerillo, A. and Taylor, S.R., 1976. Geochemistry of eocene calc-alkaline volcanic rocks from the Kastamonu area, Northern Turkey. Contributions to Mineralogy and Petrology, vol. 58, no. 1, p. 63–81.

Rimando, J., Peace, A.L., Geng, M., Verbaas, J. and Slade, H., 2022. Structural setting of the Sixtymile gold district, Yukon, Canada: Insights into regional deformation and mineralization from field mapping and 3D magnetic inversion. Minerals, vol. 12, no. 3, 29 p.

Rollinson, H.R., Rollinson, H. and Pease, V., 2021. Using geochemical data: to understand geological processes. 2nd ed., Cambridge University Press.

Rudnick, R.L., 1995. Making continental crust. Nature, vol. 378, no. 6557, p. 571–578.

Ryan, J., Zagorevski, A., Williams, S.P., Roots, C.F., Ciolkiewicz, W. and Chapman, J.B., 2013. Geology, Stevenson Ridge (northeast part), Yukon. Geological Survey of Canada, Geoscience map 116 (2nd edition, preliminary), scale 1:100 000.

Saccani, E., 2015. A new method of discriminating different types of post-Archean ophiolitic basalts and their tectonic significance using Th-Nb and Ce-Dy-Yb systematics. Geoscience Frontiers, vol. 6, no. 4, p. 481–501.

Sack, P.J. and Butty, E., (in prep). Bedrock geology map of the Sixtymile district, west-central Yukon (Parts of NTS 116C/1, 2 and 115N/15, 16). Yukon Geological Survey, scale 1:50 000.

Schmitz, M.D. and Schoene, B., 2007. Derivation of isotope ratios, errors and error correlations for U-Pb geochronology using 205Pb-235U-(233U)-spiked isotope dilution thermal ionization mass spectrometric data. Geochemistry, Geophysics, Geosystems (G3), vol. 8, no. Q08006.

Selby, D., Creaser, R.A. and Nesbitt, B.E., 1999. Major and trace element compositions and Sr–Nd–Pb systematics of crystalline rocks from the Dawson Range, Yukon, Canada. Canadian Journal of Earth Sciences, vol. 36, p. 1463–1481.

Smuk, K.A., 1999. Metallogeny of epithermal gold and base metal veins of the southern Dawson Range, Yukon. MSc thesis, McGill University, 188 p.

Souther, J.G., 1991. Volcanic Regimes. In: Geology of the Cordilleran Orogen in Canada, H. Gabrielse and C.J. Yorath (eds.), Geological Society of America, vol G2.

Staples, R.D., Gibson, H.D., Colpron, M. and Ryan, J.J., 2016. An orogenic wedge model for diachronous deformation, metamorphism, and exhumation in the hinterland of the northern Canadian Cordillera. Lithosphere, vol. 8, no. 2, p. 165–184.

Sun, S.-S. and McDonough, W.F., 1989. Chemical and isotopic systematics of oceanic basalts: implications for mantle composition and processes. In: Magmatism in the Ocean Basins, A.D. Saunders and M.J. Norry (eds.), Geological Society, London, p. 313–345.

Tempelman-Kluit, D.J., 1974. Reconnaissance geology of Aishihik Lake, Snag and part of Stewart River map-areas, west-central Yukon. Geological Survey of Canada, Paper 73-41, 97 p., (3 sheets).

Tempelman-Kluit, D.J., 1984. Geology of Laberge (105E) and Carmacks (115I) map areas, Yukon. Geological Survey of Canada, Open File 1101, scale 1:250 000.

Tempelman-Kluit, D.J., 2009. Geology of Carmacks and Laberge map areas, central Yukon: Incomplete draft manuscript on stratigraphy, structure and its early interpretation (ca. 1986). Geological Survey of Canada, Open File 5982, 399 p.

Whitney, D.L. and Evans, B.W., 2010. Abbreviations for names of rock-forming minerals. American Mineralogist, vol. 95, p. 187–187.

Winchester, J.A. and Floyd, P.A., 1977. Geochemical discrimination of different magma series and their differentiation products using immobile elements. Chemical Geology, vol. 20, p. 325–343.

Wood, D.A., 1980. The application of a Th-Hf-Ta diagram to problems of tectonomagmatic classification and to establishing the nature of crustal contamination of basaltic lavas of the British Tertiary volcanic province. Earth and Planetary Science Letters, vol. 50, no. 1, p. 11–30.

Woodsworth, G.J., Anderson, R.G., Armstrong, R.L., Struik, L.C. (Proterozoic, Paleozoic) and Heyden, P.v.d. (Coast Plutonic Complex), 1991. Plutonic Regimes. In: Geology of the Cordilleran Orogen in Canada, H. Gabrielse and C.J. Yorath (eds.), Geological Society of America, vol. G2, https://doi.org/10.1130/DNAG-GNA-G2.491.

Wynne, P.J., Enkin, R.J., Baker, J., Johnston, S.T. and Hart, C.J.R., 1998. The big flush: paleomagnetic signature of a 70 Ma regional hydrothermal event in displaced rocks of the northern Canadian Cordillera. Canadian Journal of Earth Sciences, vol. 35, p. 657–671.

Xia, L.-Q., 2014. The geochemical criteria to distinguish continental basalts from arc related ones. Earth-Science Reviews, vol. 139, p. 195–212.

Yukon Geological Survey, 2023. Yukon geochronology – a database of Yukon isotopic age determinations. Yukon Geological Survey, https://data.geology.gov.yk.ca/Compilation/22, [accessed 20/11/2025]

Zack, T., Kronz, A., Foley, S.F. and Rivers, T., 2002. Trace element abundances in rutiles from eclogites and associated garnet mica schists. Chemical Geology, vol. 184, no. 1-2, p. 97–122.